

STUDY OF CHROMIUM IN WELDING FUME

by

PRADEEP SREEKANTHAN

B.S., MASSACHUSETTS INSTITUTE OF TECHNOLOGY, 1995

Submitted to the Department of Materials Science and Engineering in Partial Fulfillment
of the Requirements for the Degree of

MASTER OF SCIENCE

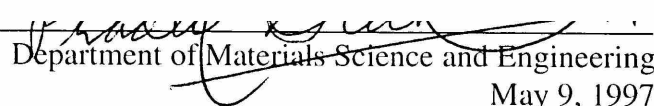
at the

MASSACHUSETTS INSTITUTE OF TECHNOLOGY

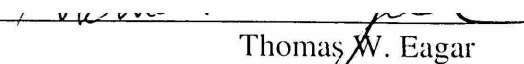
June 1997

© 1997 Massachusetts Institute of Technology. All rights reserved.

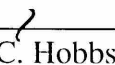
Signature of Author


Department of Materials Science and Engineering
May 9, 1997

Certified by


Thomas W. Eagar
Department Head, POSCO Professor of Materials Engineering
Thesis Supervisor

Accepted by


Linn C. Hobbs
John F. Elliott Professor of Materials
Chairman, Departmental Committee on Graduate Students
MASSACHUSETTS INSTITUTE
OF TECHNOLOGY

Science
JUN 16 1997

LIBRARIES

Study of Chromium in Welding Fume

by

Pradeep Sreekanthan

Submitted to the Department of Materials Science and Engineering on May 9, 1997, in Partial Fulfillment of the requirements for the Degree of Master of Science in Materials Science and Engineering.

Abstract

A study was undertaken to understand the influence of various shielding gases on the composition and oxidation states of various metals in welding fume. Particular attention was paid to chromium in welding fume during the gas metal arc welding (GMAW) of stainless steels. This research is part of a larger project aimed at understanding the science of welding fume, from formation to absorption by the human body. One form of chrome, hexavalent chromium (Cr VI), whose presence in welding fume is uncertain, is known to be a human carcinogen, and there are strict OSHA mandates that have reduced the permissible exposure levels (PELs) to Cr VI. Evolution of fume was observed under different shielding gas conditions. Thermodynamic calculations show that hexavalent chromium is indeed present as welding fume is evolved, but in minor amounts as it evaporates from the welding droplet. Analysis of the fume further demonstrated that Cr VI concentration is a function of the shielding gas used.

Thesis Supervisor: Thomas W. Eagar

Title: Department Head, POSCO Professor of Materials Engineering

i. Table Of Contents

i. Table of Contents3

ii. List of Tables6

iii. List of Figures5

iv. List of Abbreviations7

v. Acknowledgments8

1. Introduction 10

2. Background and Prior Work 16

 2.1 Welding Fume 18

 2.2 Effects of Exposure 19

 2.3 Fume Sources 20

 2.4 Process Variables Affecting Fume Generation 22

3. Theoretical Considerations 25

 3.1 Electrode Tip 26

 3.2 Arc Column 26

 3.3 Weld Pool 27

4. Thermodynamic Calculations 29

5. Experiments 39

 5.1 Welding Equipment 39

 5.2 Fume Collection 39

 5.3 Experimental Details 42

 5.3.1 Source of Fume 42

 5.3.2 Metals and Chrome Studies 43

 5.4 Fume Analysis 44

 5.4.1 Elemental Analysis 44

 5.4.2 Chrome Analysis 45

 5.4.3 X-Ray Photo-electron Spectroscopy 45

6.	Results and Discussion	47
6.1	Source of Fume	47
6.2	Metals and Chrome Analysis	47
6.3	Other Discussion	49
7.	Conclusions	50
8.	References	52
9.	Tables and Figures	55
10.	Appendix A: Reactants and Products in GMAW	80
11.	Appendix B: Elemental Analysis of Welding Electrodes	81
12.	Appendix C: Analysis for Welding Fume Composition	83
13.	Appendix D: NIOSH method 7600	88
14.	Biography	93

ii. List of Tables

Table 4.1	Composition of type 308 Stainless Steel	55
Table 4.2	Chemical Equilibrium in the Cr-O System	56
Table 4.3	Activities of Selected Components of Type 308 Electrodes	57
Table 4.4	Theoretical Predictions of Metal Content in Vapor	58
Table 4.5	Theoretical Calculations for Chrome Species in Vapor	59
Table 6.1	Elemental Compositions of Electrodes and Pipes	60
Table 6.2	Chemical Analysis of MS and SS Fume	61
Table 6.3	Surface Analysis of MS and SS Fume	62
Table 6.4	Chemical Analysis of Fume Samples For Metals Only	63
Table 6.5	Surface Analysis of fume Samples	64
Table 6.6	Chrome Analysis Results	65
Table 6.7	Comparison of Results with Literature	66

iii. List of Figures

Figure 2.1	Fume Formation Model for GMAW	67
Figure 4.1	Vapor Pressure for Cr (g)	68
Figure 4.2	Partial Pressures for Alloying Elements in Stainless Steels	69
Figure 4.3	Chrome Species Vapor Pressures for 99% Argon, 1% O ₂ Shielding Gas	70
Figure 4.4	Chrome Species Activities for 99% Argon, 1% O ₂ Shielding Gas	71
Figure 4.5	Chrome Species Activities for 98% Argon, 2% O ₂ Shielding Gas	72
Figure 4.6	Chrome Species Activities for 95% Argon, 5% O ₂ Shielding Gas	73
Figure 4.7	Chrome Species Activities for 90% Argon, 10% O ₂ Shielding Gas	74
Figure 4.8	Chrome Species Activities for 95% Argon, 5% CO ₂ Shielding Gas	75
Figure 4.9	Chrome Species Activities for 100% CO ₂ Shielding Gas	76
Figure 4.10	Metal Percentages in Vapor for 99% Argon, 1% O ₂ Shielding Gas	77
Figure 5.1	Fume Chamber Setup	78
Figure 5.2	Spiral Welding Bead	79

iv. List of Abbreviations

GMAW	Gas Metal Arc Welding
FCAW	Flux Cored Arc Welding
GTAW	Gas Tungsten Arc Welding
SS	Stainless Steel
MS	Mild Steel
PEL	Permissible Exposure Level
BBB	Blood brain barrier
XPS	X-Ray Photo-electron Spectroscopy
ICP-MS	Inductively Coupled Plasma - Mass Spectroscopy

v. Acknowledgments

The current project would not have happened without the support and guidance from my advisor, Prof. Thomas Eagar. I have not only gained a knowledge of joining technologies from him, but have also learned several other lessons in life. Among other things, I admire his undaunting commitment to excellence and his sparkling enthusiasm. He exudes so much confidence that I have always come out of his office charged and motivated. Moreover, I cherish the freedom given me in pursuing my research and other interests. I thank him for everything.

When the project was in its infancy, Prof. Gael Ulrich at the University of New Hampshire saved me a lot of trouble by donating their fume chamber. I appreciate his generosity, and thank him for this and his helpful discussions. His student Joe Quimby was of tremendous help in transferring the equipment. Joe sincerely responded to my SOS calls, making several trips from New Hampshire. We had very many interesting conversations and I have found a good friend in him. I wish him luck in his new career.

Prof. Joe Brain at the Harvard School of Public Health offered me the use of their facilities. I thank him for this, as also G.G. Krishna Murthy and Jim Antonini. Krishna devoted a lot of his personal time and effort to ensure that I finished my work on time, giving me valuable suggestions and insight. I am thankful to him for his support.

Edward Wu, the UROP at MIT, assisted me at crucial times. More importantly, Don Galler, our lab engineer, was available throughout the project, helping me with various things from setting up to trouble-shooting to even rides home. I thank them both, along with the rest of the Joining Group - Hilary Sheldon, Jeff Nystrom, John Matz, Renkae Shuie, Mike Zhuang, Patricio Mendez, Chris McDonald, Chris Manning, Dietmar Weiss, Sun-Woo Lee, Dongwoo Suh, and Kin-ichi Matsuyama. They helped make my days both pleasant and enjoyable – I'll certainly remember all the engaging conversations and discussions we've had.

Non-academically, life at the institute was interesting, thanks to involvement in various activities – 3.911, The-Tech, Sangam, MITHAS, just to name a few. Additionally, I had the opportunity to interact with some extraordinary people – Abhijit Sarkar, Anant Sahai, Garlen Leung, Prof. George Ruckert, Ling Liao, Neeraj Karhade, Ramdas Sunder, Ramnath Subramaniam, Sankar Sunder, Venkatesh and Rashmi Saligrama, Sumanth and Bhuvana Kaushik, T.A. Venkatesh, V.T. Srikar, Vincent Ponette, and a host of others. I value my association with them, and wish them the best in their respective endeavors.

I must mention my family, which has been supportive and encouraging of this and other pursuits. Many of them were here in Boston and I was lucky to enjoy their

company through graduate school – it was like being at home! My folks have been very understanding of me, and I appreciate each one of them – my parents, grandparents, sister, brother-in-law, nephew, uncles, aunts, cousins – for being so wonderful. I could write volumes in their praise, but I'll just end with a **BIG THANK YOU!**

There were many more who added to the present experience – the DMSE administrative staff, the Lincoln Lab - MIT shuttle drivers (Phil, Brad, Gary, and Scott) who safely ferried me to and from work everyday. I acknowledge their contributions, as well as the encouragement received from all the other unmentioned well-wishers.

This work was sponsored by the United States Department of the Navy,
Office of Naval Research.

1. Introduction

Welding productivity and weld quality have always been critical issues facing the welding community. However, extensive research has produced continuous improvements in these areas for many decades. Today welding is carried on economically and reliably, yet there are proposed standards that could dramatically reverse the progress that has been made over the past 50 years. The problem is welding fume.

Welding fume is an unwelcome byproduct of the welding process, leading to losses in worker productivity and other inconveniences. As occupational safety and health gain importance, workplace exposure comes under strict scrutiny. In the welding environment, attention is paid to welding fumes and gases. In particular, manganese and chromium, both of which are present in welding fume, are now recognized, in certain chemical states and concentrations as a neurotoxin and a carcinogen respectively.

Although there is no epidemiological data that shows that welders have greater incidences of cancer than the general population, and there is no documented case of manganism due to welding mild steels, OSHA and other organizations are proposing lowering of the PELs (Permissible Exposure Levels) of Mn and Cr by 10 to 100 fold. In the worst case, this would require welders to wear space-suit like protective equipment, and in the best case, it will severely retard productivity and greatly increase costs. For example, the estimated costs for compliance with the anticipated OSHA Cr VI standard for a PEL of $0.5 \mu\text{g}/\text{m}^3$ at Navy production facilities alone include an initial, one-time cost of about \$22 million and annual costs of about \$46 million per year (ref. 1). While this might be

considered a social problem rather than a scientific one, there are a host of scientific questions remaining to be addressed concerning the risk of Mn and Cr in welding fume.

Welding fume has recently attracted attention after reports of adverse health effects of Mn and Cr observed in other industries and processes. The OSHA standards are based upon studies of chromium in electroplating shops and manganese in paint pigments and in manganese ore mines (ref. 2). By the mid 1980's there were a number of studies underway in Europe, which prompted the International Agency on Research on Cancer (IARC) to develop the overall assessment that welding fume was possibly carcinogenic to humans (ref. 3).

In the United States, Sferlazza and Beckett described a possible association between chromium in welding fumes and lung cancer. They found an increased rate in lung cancer in welders compared with that in matched control groups. *In vitro* studies reported by Sferlazza and Beckett showed fumes from manual metal arc welding (MMAW) to be mutagenic in bioassays. However, they pointed out that epidemiological studies were unclear, since these did not separate the effects of asbestos and smoking (ref. 4). Beumont and Weiss, in a study of shipyard welders, reported an excess lung cancer mortality, but, again, they made no distinction between effects of welding fume and effects of smoking (ref. 5).

In 1989, OSHA promulgated revised mandates reducing permissible exposure limits for metal fume in half. The validity of this reduction was questioned by many who argued that it would cost US industry millions of dollars in capital and millions more per year for maintenance and operation of ventilation equipment with no proven gains in

worker health. OSHA argued that medical fees, liability suits, and lifestyle limitations attributed to welding fume were likely to cost much more (ref. 6).

OSHA's proposed standard was eventually challenged in the courts and was rejected. Many observers expected that imposition of tighter constraints is only a matter of time. Recently, OSHA has announced their intention to reduce the PEL for hexavalent chromium from the present ceiling level of $100 \mu\text{g}/\text{m}^3$, as chromates, to an 8-hour time-weighted average of between $0.5 \mu\text{g}/\text{m}^3$ and $5.0 \mu\text{g}/\text{m}^3$. The final standard is expected to be completed in 1998, with full implementation in 2000 (ref. 1).

While it is known that Mn and Cr exist in welding fume, the exact chemical form of the Mn and Cr in the fume is not understood. It may or may not be similar to the chemistry of Cr in electroplating baths and Mn in paint pigments or Mn ore dust. The toxicologists take the overly simplistic approach that it is the mere presence of a chemical element in any form that damages the body. It is known that Na and Cl are poisons, whereas NaCl is essential to life. Clearly, the chemical form and its pathway into the human body must be understood scientifically if we are to establish meaningful standards for the workplace environment. This is becoming one of the most pressing issues in welding today. Unfortunately, most people are not taking a scientific approach to the problem. This is what the following thesis seeks to address.

There is an hypothesis that manganese in welding fume, combined with iron, may not be transferred in harmful amounts across the blood-brain barrier (BBB). Work by Michael and Judy Aschner shows that Mn uptake across the BBB is modulated by plasma iron homeostasis. They have demonstrated that the Mn brain uptake levels in ferric-

hydroxide dextran-treated rats are significantly reduced compared to Mn brain levels in iron-free dextran-treated rats (ref. 7). Mn is transferred across the BBB by transferrin, which is also responsible for Fe transport. Since Fe is present in larger amounts in welding fume than Mn, the Fe molecules preferentially occupy the transferrin sites. Thus it is likely that the Fe in welding fume prevents the transport of Mn in harmful amounts across the BBB.

Oxidation is a critical factor in evaluating the activities of chromium compounds (ref. 8). Chromium exists in myriad forms and oxidation states, of which trivalent chromium (Cr III) and hexavalent chromium (Cr VI) are of interest. Cr VI is more toxic than Cr III -- its strong oxidative nature may be the underlying basis for its genotoxicity. In comparison, the trivalent state is the most thermodynamically stable (ref. 8). The majority of Cr VI that enters the body via ingestion or inhalation is quickly reduced to Cr III. Inhaled Cr VI is acted upon by alveolar macrophages (in conjunction with diverse cells throughout the lungs) and epithelial fluids within the bronchial tree. Their actions reduce the metal to its trivalent form and thereby diminish the amount of Cr VI that might enter the bloodstream after crossing the alveoli. The Cr VI that does enter the blood is reduced to Cr III by redox reactions with several blood-borne constituents and with red blood cells. Cr VI readily enters cells, penetrating the erythrocyte membrane via the general anion channel protein. Within cells Cr VI is again reduced to Cr III, in a process that is ultimately responsible for DNA damage. If Cr VI is reduced to Cr III extra-cellularly, this form of the metal is not readily transported into cells and so toxicity is not observed (ref. 9). The balance that exists between extra-cellular Cr VI and intracellular Cr III is what

ultimately dictates the amount and rates at which Cr VI can enter cells and impart its toxic effects. Therefore, any meaningful standards for chromium in welding fume should take into account the oxidation states, and must include an analysis of the various interactions within biological pathways.

To understand the chemical form of fume, a study of the evolution of welding fume under different shielding gas conditions during the gas metal arc welding (GMAW) of stainless steels is performed. The shielding gas composition is a critical process variable that influences the operation of GMAW. In the high temperature encountered in GMAW, the reactive components of the shielding gas dissociate and react with the molten metal alloy, with the result that oxygen dissolves into the metal and oxidizes certain alloying elements. The molten metal - shielding gas interactions are important in determining the reactions that lead to fume formation, and also the composition of the resulting fume. The effect of chromium and manganese as alloying elements is summarized as follows:

Chromium in amounts greater than 1% improves the oxidation resistance of the steel in high temperature applications and when present in amounts greater than 10 to 12% it makes the steel 'stainless.' The resistance of stainless steel to corrosion is due to a thin tenacious layer of chromium oxide which forms on the surface of these steels when exposed to an oxidizing atmosphere (ref. 10).

Manganese is added to the wire along with the deoxidizer silicon to aid in slag formation; although manganese is also oxidized into manganese oxide, the manganese silicate slag which forms in the molten metal separates from the weld pool more easily

than silicon dioxide alone (ref. 10). Manganese also inhibits the formation of iron sulfides.

A study of fume formation based on fundamental principles is presented. In the preceding sections, a thermodynamic model is developed, one that will allow us to predict the composition of fume from known initial conditions. Currently, the focus is limited to chromium and chromium compounds generated by GMAW of stainless steels, though the same model can easily be extended to other alloying elements and other processes as well. In the next section, background information on welding fume is reviewed along with a discussion of prior work in this area. Then, the theoretical basis for this study is presented, highlighting some of the thermodynamic calculations. The next section discusses the experiments conducted to study chromium in welding fume. Subsequently, the results and discussion section discusses the information gathered from the current research. Finally, the conclusions section summarizes current findings and suggests recommendations for future work.

2. Background and Previous Work

Several researchers have undertaken to study the evolution and composition of welding fume under different conditions, but very few have proposed models based on thermodynamic principles to explain the effect of shielding gas on fume formation, especially in chrome analysis.

Kimura, et. al, conducted an investigation of chromium in stainless steel. Their study suggested that chromium might be present in hexavalent or trivalent states and in soluble or insoluble forms, of which insoluble Cr (VI) was believed to be carcinogenic. In their analysis, they found that GMAW fume contained 15% Cr, with no Cr (VI) content (ref. 11). However, they do not report the shielding gas used, and have not considered its effect on fume formation and chrome content.

In GMAW, an inert shielding gas protects the molten electrode and work-piece from interaction with reactive atmospheric gases, such as oxygen, acts as medium in which a current can flow to sustain an arc, and affects the shape of the weld bead and resulting mechanical properties of the weldment. However, the addition of a small amount of reactive gas, usually carbon dioxide or oxygen, greatly improves the arc stability and weld penetration during GMAW. An inert gas, such as argon, used alone has been found to have unacceptable arc characteristics, bead shape and spatter, although oxygen contamination is minimized.

Shielding gas - molten metal interactions are important in determining the composition of fume. Heile and Hill were the first to conduct a major study of fume generation rates for various arc welding processes and advanced a model which predicts

fume formation rates given the consumable composition, volatility of the constituents, transfer mode, arc temperature and stability as derived from the welding parameters and shielding gas. They reported that elements in the welding electrode vaporize as droplets of the electrode are transferred through the arc to the weld pool. While welding steel, they found a disproportionately high concentration of silicon in the fume. If fume formation occurred by simple vaporization of elements in the electrode, then the concentration of silicon in fume must have been much smaller than what was reported, given that its concentration in steel and its vapor pressure are quite low. They also observed that silicon levels in fume increased with the oxygen content in the shielding gas. There were greater amounts of silicon monoxide (SiO), which is volatile, than silica (SiO₂), which is not volatile. From these results they developed a vaporization-condensation-oxidation mechanism for fume formation (ref. 12). This is elaborated in the next section.

Gray, Hewitt, and Hicks (ref. 13) confirm the effect of oxygen on the rate of fume formation in metal inert gas welding arcs. To investigate the effect of oxygen content of the shielding gas, they conducted a number of experiments with a range of oxygen contents in an argon shielding gas. They found that the fume formation rate was a direct function of the oxygen content of the shielding gas. In their experiments, the fume formation rate fell to a minimum of 0.22 g/min when the shielding gas was pure argon, for a variety of stainless steel welding wires, compared with values ranging up to 0.4 g/min when the shielding gas contained 4 volume-percent oxygen (ref. 13).

The current work is also based on previous research in our laboratories: Gibson considered elemental transfer for 0.07 carbon MIL-140S type wire to HY 130 steel under different shielding gas conditions. She developed the ability to predict, from basic thermodynamic relationships, elemental transfer rates through the arc for GMAW over a wide variety of initial alloy chemistries and shielding gas compositions. Using this framework, it was possible to calculate the final weld pool chemistry knowing only the initial electrode, plate, and gas compositions (ref. 14). The current research extends the application of these concepts to fume studies.

Block-Bolten and Eagar conducted an analysis of metal vaporization from arc weld pools using a similar approach based on thermodynamic data. They concluded that Mn and Fe were the dominant vapors when welding steel and stainless steel, with a maximum weld pool temperature of 2500°C (ref. 15). This model of weld pool vaporization will now be extended to fume studies to include interactions in the arc column under different shielding gas conditions.

Some relevant background information will be reviewed, along with pertinent investigations, before the details of the current research are presented.

2.1 Welding fume

The American Welding Society defines fume as the particles formed by electrode (and base metal) that are vaporized and subsequently condensed in the welding area (ref. 16). In fact, any material when heated to high temperatures is a potential source of fume. Welding fume is produced whenever a material which is normally solid at room

temperature, such as metal in the welding consumable, is heated near its boiling point and the vapors condense, react, oxidize or coalesce to form a dispersion of fine airborne solid particles. During welding, most of the consumable electrode is deposited onto the base plate, however, a small portion (on the order of one percent) is emitted to the atmosphere as fume. The fume generation rate, composition (and potential toxicity), morphology and particle size, all vary depending on the welding conditions and materials involved. In general, fume formation involves the thermodynamics of vaporization of metals from the molten electrode, the agglomeration of respirable size particles, their oxidation in the atmosphere, and the solubility of these particles in the lungs and gastro-intestinal tract (ref. 3).

The vaporized metal condenses into very small particles that remain in the aerosol form for extended periods of time. These particles have mass and size, so they are affected by air movement, electric fields, gravity, diffusional forces, and other external forces. They tend to agglomerate into clumps that generally settle down. However, while they are suspended they are inhaled by the welder and all others in the vicinity (ref. 16)

2.2 Effects of Exposure

The degree of hazard to the welder depends on the composition of the fumes and their concentration in the air that is breathed. Welding fume normally enters the body through inhalation. Once in the lungs, it can remain there or be absorbed into the blood stream. Inside the body, each material initiates different and specific effects.

Sferlazza and Beckett observed acute effects (those that develop shortly after exposure and do not last very long) in welders that included airway irritation, acute bronchitis, metal fume fever (attributable mainly to zinc) (ref. 4). None of these diseases can be attributed to the chromium content in fume. Chronic respiratory effects reported were chronic bronchitis, pneumoconiosis, fibrosis, and, as mentioned earlier, certain incidences of lung cancer. They recorded a presence of substances in welding fume that are known to cause excess lung cancer in other occupations (ref. 4). Chromium in welding fume was labeled as possibly carcinogenic following studies dealing mostly with workers in the chromate production industry, chromate pigment workers, and workers in the chrome-plating and ferro-chrome industries (ref. 9). Furthermore, it was not possible to pinpoint welding fume as the causative agent for cancer since welders are also exposed to asbestos and cigarette-smoke, both of which are confirmed carcinogens (ref. 4).

Antonini, et. al, studied the pneumotoxicity and pulmonary clearance of different welding fumes in rats. They found a greater retention of stainless steel (SS) spray particles from GMAW compared to mild steel (MS) spray and MS-pulsed welding. They concluded that SS fumes were more toxic than MS fumes. However, the pulmonary fate of the particles generated during welding and the potential of these particles to induce lung injury and inflammation are largely unknown (ref. 17).

2.3 Fume sources

In GMAW, the primary sources of welding fume are the electrode, the base plate, and surface coatings, if any. Figure 2.1, illustrates gas-shielded welding on an uncoated

metal, highlighting the potential sources of fume. According to Gray, Dewitt, and Dare, fume comes from droplet evaporation, the weld pool, electrode spots, the exploding wire, deflected droplets, fume metal droplets ejected by wire explosion, and from the molten weld bead (ref. 18).

Ulrich identifies similar sources, as in figure 2.1, for fume formation, with a few modifications. The droplet at the electrode tip is believed to contribute to fume via two mechanisms, droplet evaporation and arc-root evaporation. Droplet evaporation is defined as the diffusion of metal from all surfaces of the molten droplet other than the arc-root, while the arc-root evaporation simply refers to diffusion of metal from the arc-root, which is the part of the droplet heated by the electric arc. Ulrich considers droplet evaporation to be insignificant relative to arc-root evaporation because the droplet temperature is much lower at surfaces other than the arc-root. Looking at other mechanisms, he disregards the weld pool and bead as fume sources since they are clean and at much lower temperatures. He observes that GMAW occurs under low-spatter conditions, so ejected metal particles are also not significant in fume formation. He summarizes that the most important mechanisms for fume formation are thus arc-root evaporation and explosive evaporation (the violent ejection of droplets into the gas phase) (ref. 6).

Castner points out that most of the fume comes from the electrode, with hardly 10% coming from the base metal (ref. 19). Voitkevich reports that the drop on the electrode is the main source of welding fume because the drop stage is characterized by a high specific surface (an order of magnitude more specific surface area than the weld

pool) and by a higher level of overheating (ref. 20). Voitkevich and others (ref. 20, 12) performed gas tungsten arc welding (GTAW) using an inert electrode and found no fume even after the arc melted the base-metal. From this they concluded that the electrode, and not the weld pool, was the source of fume. However, the same cannot be said about of GMAW since this would be a comparison of two entirely different processes. Instead, reference is made to Heile and Hill who conducted experiments on Mg bearing Al plates to determine the source of fume. They used two types of electrodes -- type 5356 containing Mg and type 1100 containing no Mg. Mg was found when the 5356 electrodes were used, but no Mg was found when the 1100 electrodes were used, even though the base metal contained Mg. From these results, they conclude that most of the fume comes from the electrode tip and the welding arc, with insignificant quantities from the weld pool (ref. 12). Independent tests were performed, as discussed later on, to verify for ourselves the source of welding fume.

2.4 Process variables affecting fume generation

A number of researchers have studied the effects of major process variables on fume generation rates (ref. 19, 12, 20, 17). These include welding conditions (such as current and voltage), electrode composition, electrode diameter, work-piece travel speed, mode of metal transfer, and shielding gas composition.

Fume generation rate usually increases with an increase in current, unless one is at the transition region from globular to spray transfer, where there is a decrease in fume generation (ref. 19, 21). As current is increased, the arc temperature is increased,

vaporizing more of the metal. Additionally, the melting rate of the electrode is increased with higher currents, which leads to more material passing through the arc per unit time, thereby, resulting in increased fume (ref. 19). The exact behavior of fume as a function of current, however, depends on the choice of shielding gas. Castner reports a steady linear increase for CO₂ (ref. 19), while argon-based mixtures show a more complicated behavior (ref. 19, 21).

With an increase in voltage, fume generation increases again. This follows from the fact that an increased voltage leads to a lengthened arc, which results in molten drops spending more time in the air, increasing the molten metal-gas reactions (ref. 19).

Shielding gas composition, welding current, and arc voltage influence the mode of metal transfer, and, therefore, the size and temperature of the metal droplets transferred through the arc, the time for the droplet to transfer through the arc, and the degree of spatter, which in turn affects fume formation (ref. 19). For short circuit transfer (metal transfer during a period when the electrode is in contact with the work-piece), which occurs at low welding currents and low voltages, fume generation is low. An increase in welding current and voltage results in more metal deposited, signaling the onset of globular transfer (characterized by a drop larger than the electrode diameter, easily acted upon by gravity). Spatter increases and with it fume generation rates. Castner reports that with CO₂ shielding gas, the fume generation rate increases with current and voltage, while in an argon-based shielding gas, there is an eventual transition to spray transfer (ref. 19). During spray transfer, transfer occurs in the form of very small drops that are formed and detached at the rate of hundreds per second. This transition results in a decrease in

spatter and fume levels. According to Heile and Hill, this reduction is due to a dramatic decrease in the surface area of molten drops exposed to the arc (ref. 12). While operating in the spray mode in argon-based shielding gases, there is an increase in fume formation with increases in welding current and voltage.

Considering other variables, Heile and Hill studied the effects of work travel speed and found no appreciable influence on fume generation. They found that increasing the travel speed by a factor of two only resulted in a 5% reduction in fume (ref. 12).

3. Theoretical Considerations

It is often mistakenly believed that the dominant specie in the consumable is also the dominant specie in metal vapor or in welding fume. However, this is not the case since the system contains various substances with different vaporization potentials and volatile natures. These materials vaporize under different conditions. Fume formation is not so simple and is presented as a two-step process. The first is elemental vaporization, wherein the elements in the welding electrode vaporize from the droplets of the electrode as they are transferred through the arc to the weld pool. Other researchers suggest that more volatile compounds are concentrated more heavily in the gaseous phase and that elemental vaporization alone does not account for all the constituents in fume (ref. 12, 15). The presence of oxides in fume suggests that oxidation of the fume in the air might be important, so the second process is oxidation-enhanced vaporization. The complete picture of fume formation is therefore given by a vaporization - condensation - oxidation model.

Our objective in this study is to develop a predictive capability for chrome content in welding fume, given the shielding gas composition. This can be obtained from known initial conditions through a consideration of a thermodynamic model of the reactions occurring in GMAW. Our concern is the molten metal - shielding gas reactions that take place. The reaction conditions in the welding process are dependent on the locations of the reaction. Prior researchers have established that the areas of importance are the electrode tip, the arc plasma column, and the weld pool (ref. 22, 23, 24). The molten

metal - shielding gas interactions in each of these areas are reviewed, after which are presented the thermodynamic calculations used to model fume formation.

3.1 Electrode Tip

As the electrode melts into molten droplets at the electrode tip, what is seen is the vaporization of the metal and dissolution of oxygen into the molten metal. Fume is generated by the vaporization of the elemental metals. Additionally, metal oxides are also created by the addition of oxygen to the metallic elements, thereby contributing to fume generation. The continuous introduction of the solid electrode keeps the tip cool as droplets enter the arc plasma column. Other researchers claim temperatures reaching 2000°C (ref. 14). Jones explains the presence of a temperature gradient along the vertical axis of the melting droplet, given the large size of the droplet: Near the bottom of the drop the temperature is found to be approximately 2200° C, at the equator 1950° C, and the liquid/solid interface approximately 1600° C (ref. 25). As the drop detaches from the electrode tip, it enters the arc plasma column. Its temperature is now close to the maximum temperature permitted by the balance between the heat input from the arc and the evaporative cooling due to metal vaporization.

3.2 Arc Plasma Column

There are conflicting reports as to what reactions occur in the arc plasma column. Grong and Christensen claim that vapors of iron and manganese envelop the molten

droplet throughout the arc plasma column, preventing any further reactions (ref. 22). However, Gedeon and Rudd suggest that oxygen pickup does continue past the electrode tip and throughout the droplet's course through the arc plasma column (ref. 26). Thus, in the arc plasma column, the relevant reactions are the continued dissolution of oxygen from the ionized shielding gas into the droplets and the reaction of this oxygen with the various metals in the steel to form metal oxides (ref. 14). Measurements of average temperatures of the transferring drop, made with calorimeters, give results between 2000° C and 2700° C (ref. 27). However, measurements of drop temperatures by direct impingement on a thermocouple suggest agreement with the evaporation cooling limit of 2400° C (ref. 27).

3.3 Weld Pool

The weld pool can be seen as two portions, the hot and the cool. In the hot portion, the reactions of relevance are the same as those occurring in the arc plasma column. According to Grong and Christensen, no further oxygen absorption occurs here (ref. 22). However, Francis et. al disagree and suggest that a good portion of the gas-metal reactions occur in the weld pool because a negative oxygen content in the transferred droplets is calculated for low oxidizing shielding gases if such is not the case (ref. 28). According to Gedeon and Rudd, the hot and cool areas of the weld pool exhibit turbulence, allowing the system to tend toward thermodynamic equilibrium concentrations of alloying metal and residual gases under the weld pool conditions (ref.

26). Block-Bolten and Eagar suggest a model of selective evaporation of metals from weld pools based on thermodynamic data and the kinetic theory of gases, recognizing that the dominant specie in the weld pool was not the dominant specie in the metal vapor. They calculate a maximum weld pool temperature of 2500°C (ref. 15), though Grong and Christensen record much cooler temperatures (ref. 22).

The exact location of the molten metal - shielding gas reactions has been observed to depend on the choice of shielding gas and resultant droplet behavior (ref. 12, 18). For CO₂-based shielding gases, metal transfer occurs by globular transfer. The droplet grows at the tip of the electrode, usually until it is significantly larger in diameter than the electrode, then becomes detached and falls into the weld pool (ref. 18). The droplet spends a larger amount of time on the electrode tip than it spends in the arc column (ref. 29). For Ar-based shielding gases, transfer occurs by the spray mode. Very small drops form and detach at the rate of hundreds per second. The drop spends far less time at the tip of the electrode; drop volume decreases rapidly, while the rate of transfer increases (ref. 12). The drop detaches from the electrode and passes through the arc column, which is the dominant region for the vaporization-condensation-oxidation process.

4. Thermodynamic Calculations

The topic to be addressed is the molten metal-shielding gas reaction. This situation can be elegantly modeled using the tool of thermo-chemical analysis. Thermo-chemical analysis allows us to evaluate the oxidizing potentials of reactive gas mixtures, the thermo-chemical stability of condensed metal and oxide phases, and the equilibrium pressures of volatile species over the condensed phase (ref. 30). These are a function of temperature and oxygen content of the gas mixtures.

With an understanding of the thermodynamics, various quantities such as final molar fractions for different shielding gas mixtures can be determined and applied to fume composition calculations. To keep the model simple, flexible, and accurate, thermodynamic equilibrium for the gas-metal reactions will be assumed in the following computations.

Thermo-chemical analyses use free energy data, ΔG° , and equilibrium constant data, $\log K_p$. The basic equations for deriving and using thermo-chemical data is as follows:

$$\Delta G^\circ = -RT \ln K_p \quad 4.1$$

Equation 4.1 is the expression for the standard Gibbs free energy ΔG° in terms of the equilibrium constant K_p (ref. 30).

Thermo-chemical data for elements, compounds and vapor species have been collected in numerous publications like the JANAF tables. More recently, computer techniques have eased thermo-chemical analysis, as demonstrated later on.

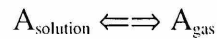
For a pure metal A, the free energy of evaporation, ΔG°_e , is given by:

$$\Delta G^\circ_e = -RT \ln P^\circ_A \quad 4.2$$

where R is the gas constant, T the absolute temperature (in Kelvin) and P°_A is the equilibrium vapor pressure of pure A at temperature T.

Values for ΔG°_e are tabulated for a range of temperatures. Hence, given a temperature, the equilibrium vapor pressure can easily be obtained. In figure 4.1, we use equation 4.2 and tabulated values of from *HSC Chemistry's* (a thermodynamic software package describe later on) database to plot the equilibrium vapor pressure as a function of temperature for the reaction $\text{Cr (s,l)} \rightleftharpoons \text{Cr (g)}$.

If A is not pure, but is in solution, the free energy change on evaporation is given by $\Delta G^\circ_e - \overline{\Delta G}$, where $\overline{\Delta G}$ is the partial molar free energy of mixing of A for the reaction



From equation 4.1, we know that

$$\overline{\Delta G} = -RT \ln \overline{P}_A \quad 4.3$$

where \overline{P}_A is the partial pressure of A above the alloy.

When metal A evaporates from an alloy, the total free energy change is then given by subtracting equation 4.3 from equation 4.2 to obtain:

$$\Delta G^\circ_{\text{tot}} = RT \ln (\overline{P}_A / P^\circ_A) \quad 4.4$$

The term $(\overline{P}_A / P^\circ_A)$ is defined as the thermodynamic activity, where we can use the expression:

$$\ln \bar{P}_\Lambda = \ln P^\circ_\Lambda + \ln a_\Lambda \quad 4.5$$

That is, the (natural) logarithm of the partial pressure of an alloy component in the gas phase is proportional to the sum of the logarithms of the standard pressure of the pure element and the activity of the element in the alloy.

If the composition of the metal is known, the activity for an element can be obtained from Hultgren's tabulated values for binary melts (ref. 31). These numbers are strictly for binary melts, however, in the absence of strong interactions between atoms, the data can be used to approximate a more complex alloy (ref. 15). Hultgren's activity data (a_o) are recorded for a particular temperature, T_o . These values can be extrapolated to other temperatures, T_n , using the following relationship:

$$\log a_n = \log a_o + \frac{\overline{\Delta G^{xs}}(T_o - T_n)}{4.575 T_o T_n} \quad 4.6$$

where $\overline{\Delta G^{xs}}$, the partial excess free energy of mixing, can also be obtained from tabulated values (ref. 31).

Using the above equations, it is possible to calculate the vapor pressures for alloying elements in any typical alloy. Figure 4.2 is a plot of the partial pressures for different alloying elements in various stainless steel compositions. As seen in the figure, manganese and chromium have high vapor pressures in the temperatures of interest, which explains their volatile behavior. Mn and Cr evaporate sooner than other elements present in the electrode. Therefore, their concentration in fume is greater than their concentration in the welding consumables.

These calculations have only dealt with elemental vaporization from the alloys. To model fume formation in its entirety, oxidation-enhanced vaporization also needs to

be considered. The following calculations are performed for stainless steels, using type 308 (whose composition is given in table 4.1) as an example (the same electrode has been used in the experiments). It is just as easy to apply these concepts to other alloys as well. The focus of this study is chromium, so the current calculations are limited to chromium and chrome oxides, though the same model can easily be extended to other alloying metals as well. Table 4.2 shows the chemical equations for the Cr-O volatile species above the condensed phases Cr (s,l) and Cr₂O₃ (s,l). Volatile species are formed by direct evaporation and by the addition or removal of oxygen from Cr (s,l) and Cr₂O₃ (s,l) respectively.

Fume formation involves the evolution of the gaseous species listed in the table. Elemental evaporation of Cr (g) has already been considered. For the reactions involving the evolution of the oxide species, reference is made to equation 4.1, the free energy equation:

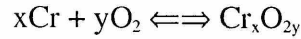
$$\Delta G^\circ = -RT \ln K_p \quad 4.1$$

For these reactions the mass action constant can be expressed as:

$$K = \prod (a_{\text{products}})^{\text{coefficients}} / \prod (a_{\text{reactants}})^{\text{coefficients}} \quad 4.7$$

For gases, the activities are represented by the equilibrium partial pressures. The activity of the reacting liquid metal can be obtained from Hultgren's tables looking up a Fe-Cr binary alloy (ref. 31). For 308 steels, with a chromium content of 20.5 % by weight, the activity is calculated to be 0.315. The activities for some of the alloying elements in this steel composition is given in table 4.3. The coefficients in equation 4.7 vary depending

on the reaction in consideration. For a general oxidation of Cr, the reactions can be written as:



Equation 4.7 then becomes:

$$K = P_{\text{Cr}_x\text{O}_{2y}} / (P_{\text{O}_2})^y / a_{\text{Cr}}^x \quad 4.8$$

For this system, equation 4.1 can be rewritten as:

$$\ln (P_{\text{Cr}_x\text{O}_{2y}} / (P_{\text{O}_2})^y / a_{\text{Cr}}^x) = - \Delta G^\circ / R / T \quad 4.9$$

From equation 4.9, the vapor pressure of the chromium oxides is a function of temperature and also the partial pressure of oxygen, which is given by the oxygen content in the shielding gas (typically argon-based). For a pure argon shielding gas, there is no oxygen present in the shielding gas, so one would expect only Cr(g) in the fume during formation. With an addition of 1% oxygen in the shielding gas mixture, $P_{\text{O}_2}=0.01$. Using this value in equation 4.9, activities (vapor pressures for gases) for the chromium species are plotted as a function of temperature, as shown in figure 4.3. From this figure, it is possible to identify the dominant specie for any given temperature - e.g. at 2400° C Cr (g) is the dominant form. We notice that for CrO₂ (g) and CrO₃ (g) an increase in temperature is accompanied by a decrease in vapor pressure, whereas for Cr (g) and CrO (g), there is a increase in vapor pressure with temperature.

Cr (g) is representative of elemental vaporization. The oxides represent the various valencies of chrome in fume. That is, the presence of CrO signals Cr II, Cr₂O₃ shows Cr III, CrO₂ Cr IV, and finally CrO₃ Cr VI. The specific amounts of these compounds depends on the oxygen partial pressure as seen in equation 4.9, which

suggests that the valency of chromium varies with the oxygen potential of the shielding gas.

The treatment so far has considered chromium and oxygen as the only components of the system. However, the welding atmosphere is actually a multi-component system. The presence of several alloying elements with different properties leads to numerous reactions occurring simultaneously and / or in competition with one another. This represents a more complex situation since there are multiple equilibria to model. Fortunately, the task is simplified with the aid of a personal computer and appropriate thermodynamic software.

This study uses *HSC Chemistry for Windows* by Outokumpu Research Oy, Finland. The *equilibrium compositions* subroutine is evoked to analyze multiphase equilibrium compositions easily in the heterogeneous system, represented here by the molten metal - shielding gas interactions. The user specifies the reaction system and gives the amount of raw materials and the program calculates the amounts of products at equilibrium. The program takes as inputs molar quantities and activity coefficients of the reacting species and outputs equilibrium values for the entire system.

The analysis begins by specifying the elemental compositions of the electrode and shielding gas, from which is generated a list of all the reacting species and resultant products. Appendix A contains such a list for GMAW of 308 stainless steels using argon-based shielding gases. The molar quantities of the species involved in the molten metal - shielding gas reactions depend on the welding parameters. The amount of molten metal available for reaction is a function of electrode diameter and wire feed speed, while

the amount of shielding gas is governed by the gas-flow rate. Calculations are therefore made for a fixed time period recognizing that some variables are time-dependent quantities.

From the electrode diameter and wire feed speed, the amount of electrode consumed is obtained using the following relationship:

$$\begin{aligned} \text{Amount of electrode} &= (\text{Time}) \times (\text{Volume of electrode/Unit time}) \times (\text{Density}) \\ &= (\text{Duration of weld}) \times (\text{Wire feed speed}) \times (\text{Cross-sectional area}) \times (\text{Density of electrode}) \end{aligned}$$

The duration of welding is known, as also the wire feed speed. The cross-sectional area can be calculated from the electrode diameter. Density of the alloy is easily found in tabulated sources like the Metals Handbook (ref. 10), etc. The relationship outlined above gives the weight of the electrode consumed, from which it is possible to determine the molar quantities of the constituents since the weight percent of the alloy is already known (table 4.1).

The activity coefficient for substance i is defined as the ratio of activity to concentration:

$$\gamma_i = a_i / x_i \quad 4.10$$

It has earlier been shown how activities can be obtained as a function of temperature.

The activity coefficients are calculated in an identical fashion, except for a minor modification to equation 4.6 that now includes the concentration term in the denominator of equation 4.10:

$$\log \gamma_n = \log \gamma_o + \overline{\Delta G^{ss}} (T_o - T_n) / (4.575 T_o T_n) + \log x_i \quad 4.11$$

Equation 4.11 is then entered for each of the alloy components.

For the shielding gas, calculations proceed as follows. The volume of gas that is consumed is found by multiplying the duration of welding by the gas-flow rate. Molar quantities are calculated by simple extension of the ideal gas law:

$$n = PV / RT \quad 4.12$$

The fraction of each component is given by the gas composition. Equation 4.10 is used for activity coefficients, where a_i is the partial pressure of the gas, which is its percentage in the shielding gas composition.

The program is instructed to make calculations for temperature increments between 1500° C and 2700° C – a broad range of temperatures that includes typical droplet / weld-pool temperatures. Total pressure is assumed to be 1 atmosphere. Once the relevant data are entered, the computer calculates equilibrium compositions using the Gibbs Energy Minimization Method. The program finds the most stable phase compositions where the Gibbs energy of the system reaches its minimum at a fixed mass balance (a constraint minimization problem), constant pressure and temperature.

The vapor pressures for the chrome system are now obtained recognizing that the chrome reactions are actually occurring in a multi-component system. Figures 4.4 through 4.7 show the equilibrium activities (vapor pressures for gases) as functions of temperature for a variety of argon-based shielding gases with different oxygen contents. Figure 4.4 is for 1% oxygen (this is figure 4.3 now recast in a multi-component system), figure 4.5 for 2% oxygen, figure 4.6 for 5% oxygen, and figure 4.7 for 10% oxygen. Since carbon dioxide may also be used in place of oxygen in the shielding gas, figures 4.8

and 4.9 consider the equilibrium activities for gas compositions of 95% argon - 5% carbon dioxide, and 100% carbon dioxide respectively.

The trend is as before. Cr (g) is the dominant form in the chrome system. Cr VI, in the form of CrO₃ (g) has the lowest activity among the gaseous species.

The advantage of the computer program is the ability to predict relative amounts of the products. In figure 4.10, the amount of vaporized metal as a fraction of the total vapor in the products is given for a shielding gas composition of 99% argon, 1 % oxygen. The percentages are plotted as a function of temperature. Table 4.4 lists the percentages of metals in the vapor during formation for 2400° C, the theoretical droplet temperature, as explained earlier. The table lists these percentages for all the shielding gases considered in this study. The table shows that iron is the dominant metal although there are also significant amounts of chromium and manganese as well.

Considering only the chrome system, it is possible to identify the amounts of the different species in the vapor. This is shown in table 4.5 for 2400° C, though it is as easy to calculate these percentages for other temperatures. One notices that Cr (g) is the dominant form for all gas compositions. CrO₃ (g), and hence Cr VI, is found only in very small amounts, about 1.30E-4 % of total vapor, or 5.00E-4 percent of the chrome content. As oxidizing potential increases, there is an increase in the CrO₃ (g) content, although this is very small – as seen from the table, a 900% increase in the oxygen content sees hardly a 1% increase in the CrO₃ (g) content.

This model has only predicted percentages during fume formation. However, upon formation these particles are exposed to air and are subject to further oxidation.

Oxidation will change the composition of fume. This composition can easily be obtained by conducting appropriate experiment. However, there is no theoretical tool available to predict these numbers earlier by simple calculations. What is now required is a model that will correlate the percentages calculated by the model of fume formation to those obtained via experimentation.

Furthermore, the aforementioned calculations have only included the reactions occurring on the droplet surface. As has been explained earlier, other parts of the droplet are at much lower temperatures than the surface, and, hence, the reactions occurring here are not believed to participate in fume formation. Additionally effects of the arc plasma, where the diatomic gas molecules disassociate to monatomic forms, have not been considered. This consideration requires modeling of a partially-ionized arc plasma column, a system that is not completely understood. A more thorough investigation will have to include these influences also, but is beyond the scope of the current study.

5. Experiments

The focus of the experiments is two-fold. The first is to verify the source of fume in GMAW, while the second is an analysis of chrome evolution during GMAW under different shielding gas conditions.

5.1 Welding Equipment

GMAW is performed using a Hobart Arc-Master 500 power supply and a Hobart 2410 semiautomatic solid-state control wire feeder (Hobart Brothers, Troy, OH). The Arc-Master 500 is a primary inverter power source current-rated at 500 amperes / 40 volts at 100 % duty cycles, and is suitable for all modes of operation. The 500 can support GMAW, steady and pulsed, as well as SMAW and FCAW.

A constant voltage of 30 volts and a wire feed speed of 300 inches per minute (127 mm/sec) is maintained for the experiments, and the equipment is operated in DCEP polarity. The corresponding current is recorded for each weld. Shielding gas is supplied at a steady rate of 50 cubic feet per hour. Throughout the experiments it is necessary to maintain these constant welding conditions since varying welding parameters can appreciably influence fume formation.

5.2 Fume Collection

Experiments are performed in a fume chamber specially designed by Ulrich and coworkers at the University of New Hampshire (ref. 32). An important consideration in

this design has been the desire to operate a welding torch at steady-state for extended periods of time. This suggests the use of a cooled rotating pipe as the work-piece rather than a disc as recommended by the American Welding Society standards (ref. 33). A stock cylindrical pipe, about 25 cm. in diameter (10 inch, schedule 40) by 30 cm. long, is used. The pipe is encased by a chamber, constructed by welding together two large bottomless pressure cookers. Figure 5.1 shows this setup. As illustrated, the pipe rotates as though it were in a lathe. The chamber moves horizontally along the same axis as the work, much as the cutting bit traverses the work-piece in a lathe. Both rotational and linear motion are independently controlled by two separate stepper motors (ref. 32). For the experiments, rotational motion was set at 0.42 revolutions per minute, corresponding to a linear work-piece travel speed of 14 inches per minute as recommended by the American Welding Society (ref. 33).

The weld gun is attached to the chamber. An auto-darkening lens is installed beside the welding port to allow observation. The weld bead is laid on the enclosed pipe, forming a spiral as shown in figure 5.2. Cooling is achieved via room air which flows through the supporting shafts. Cooling water or metered air can also be used. The same rotating shaft also acts as the ground path with a Tweeco™ ground-union attached at the free end.

Metal fume is collected by creating a negative pressure in the chamber using a *Omega Vac* self-contained fine filtration vacuum (Atrix International, Burnsville, MN), equipped with high efficiency filters to trap small particles. HEPA (High Efficiency Particulate Air) filters (Atrix International, Burnsville, MN), with a labeled efficiency of

99.67 % at 0.12 microns, are used. As particles collect in these filters, the vacuum cleaner becomes less efficient, thereby reducing the flow-rate of air through the chamber. The flow rates were monitored using a *Magnehelix* water pressure gauge (Dwyer Instruments Inc., Mich. City, IN), which was later on calibrated using a Model 1440 digital air velocity meter (Kurz Instruments Inc., Monterey, CA). Flow rates through the exhaust dropped from approximately 1700 liters per minute to values around 700 to 800 liters per minute.

Fume exits the chamber through the exhaust located on the top of the chamber. The exhaust houses the filter holder, where appropriate filters collect fume from the exhaust stream. These filters are connected to a vacuum pump (GAST Manufacturing Corp., Banton Harbor, MI) that maintained a flow rate of around 3 liters per minute. Three different filters were used for each weld. Nuclepore membrane filters, 37 mm in diameter, with a pore size of 0.2 μm (Corning-Costar, Cambridge, MA) were used to collect fume for elemental analysis. PVC membrane filters, 37 mm in diameter, 0.8 μm pore size (FKC, Eighty Four, PA, through DataChem Labs, Salt Lake City, UT) were used to collect fume for chrome analysis. MCE filters, 37 mm in diameter, 0.2 μm pore size (FKC, Eighty Four, PA through DataChem Labs, Salt Lake City, UT) were used to collect samples for analysis by x-ray photo-electron spectroscopy (XPS). Sampling was begun after the arc was struck and steady state conditions established. The sampling time was 3 minutes to allow sufficient collection for the various analyses.

5.3 Experimental details

Two sets of experiments are reported:

1. Those conducted to verify the source of welding fume.
2. Those performed to study the influence of shielding gas composition on the metal and chrome content in fume

5.3.1 Source of fume

The electrode and work-piece compositions were respectively changed to analyze the source of welding fume. Weld beads were laid on the rotating pipes (work-pieces) according to the following scenario:

1. Stainless steel (SS) electrode, 0.045 inches diameter, type 308 (McKay, Troy, OH) on SS pipe, type 304/304L (Stainless Pipe and Fittings, Randolph, MA).
2. Mild steel (MS) electrode, 0.045 inches diameter, type ER70S-3 (Hobart, Troy, OH) on SS pipe.
3. MS electrode on MS pipe, type A500 (Novel Iron Works, Greenland, NH).
4. SS electrode on MS pipe.

The evolved fume was collected for each weld for elemental analysis on Nuclepore filters with a pore size of 0.2 microns. A low pore size was chosen so as to capture most fume, where the average respirable particle size ranges from 0.1 μm to 5 μm (ref. 20). These filters were analyzed by the Trace Metals Lab at the Harvard School of Public Health, Boston, MA. Elements of interest were Fe, Cr, Ni, Mn, Cu, Co, and Mo. For this set of

experiments the shielding gas mixture remained unchanged at 98 % argon, 2 % oxygen, which is a common GMAW composition.

5.3.2 Metals and Chrome Studies

A key motivation for this research has been the desire to conduct a study of chrome evolution under the influence of different shielding gas conditions. In the previous section, the theoretical approach to solve this problem was presented. Now the experimental details are provided.

For this set of experiments, GMAW was performed on SS pipes, type 304/304L (Stainless Pipe and Fittings, Randolph, MA) using type 308 SS electrodes (McKay, Troy, OH), 0.045 inches in diameter. Welding was done under different shielding gas compositions, from totally inert to highly oxidizing. Five compositions were used: 100 % argon, 98 % argon and 2 % oxygen, 95 % argon and 5 % oxygen, 95 % argon and 5 % carbon-dioxide, 100 % carbon-dioxide. For each shielding gas composition, experiments were conducted under two chamber conditions. First, house air was allowed to flow through the chamber. This situation is similar to actual shop conditions and the fume collected on the filters is expected to be identical to the fume inhaled by workers. Subsequently, the chamber was flushed with argon, and a constant flow of the inert gas was maintained without creating any positive pressures in the chamber. Under this condition, the fume is not expected to undergo any further reactions after it exits the arc column, so the fume that is collected is similar in composition when formed.

Fume was collected, for each run, on 3 different filters – Nuclepore membrane for elemental analysis, PVC membrane for chrome analysis, and MCE membrane for XPS analysis.

5.4 Analysis

Fume was collected on appropriate filters for analysis for three different purposes -- elemental analysis, chrome analysis, and XPS. The electrodes were also analyzed for elemental composition.

5.4.1 Elemental Analysis

A. Electrode

The electrodes used for the experiments were analyzed for their compositions. Analysis was performed by Luvak Inc. of Boylston, MA, where oxygen content was determined by inert gas fusion, carbon was analyzed by combustion / infrared detection, and the remaining elements were analyzed by direct current plasma emission. Details of the tests are given in Appendix B.

B. Fume

Fume for elemental analysis was collected on Nuclepore filters, as described earlier. These samples were analyzed, using chemical and spectroscopic techniques, by the Trace Metals Lab at the Harvard School of Public Health, Boston, MA. The procedure involved was as follows: Gravimetric analysis was performed on the filters

prior to digestion by the sediment microwave digestion technique. Sample extracts and digestates were analyzed for metals using Inductively Coupled Plasma - Mass Spectroscopy (ICP-MS). More details on this analysis can be found in Appendix C.

5.4.2 Chrome Analysis

Welding fume was collected on PVC membrane filters for analysis of the chromium content, specifically hexavalent chrome. These filters were shipped to DataChem Laboratories in Salt Lake City, UT, a NIOSH- (National Institute for Occupational Safety and Health) certified facility, where they were analyzed using NIOSH method 7600, a chemical / spectroscopic procedure for determining Cr VI content. This method involves digestion of the filters, followed by spectroscopic analysis of the digestate. Appendix D outlines the steps involved in this test.

5.4.3 X-Ray Photo-electron Spectroscopy

X-ray photo-electron spectroscopy (XPS) was conducted to obtain information about the surface composition of welding fume. XPS was performed at the Gordon-McKay Labs at Harvard University, Cambridge, MA, using a SSX-100 ESCA Spectrometer (Surface Science Laboratories, Mountain View, CA). XPS, also known as ESCA, is based on the interaction between the substances in fume and electromagnetic irradiation. Any particular substance absorbs a quantum of electromagnetic irradiation where the quantum of energy is equal to change in energy of a molecular or atomic process. XPS was used to obtain the relationship between the energetic position of

electron spectrum lines and types of chemical bonds and compounds. Specific attention was paid to the spectral lines corresponding to Cr and Cr oxides in an effort to distinguish between different species and their relevant amounts in welding fume.

6. Experimental Results and Discussion

6.1 Source of fume

GMAW was performed on SS pipes using SS and MS electrodes, and subsequently on MS pipes using MS and SS electrodes. Table 6.1 lists the compositions of the electrodes and base-metal used. The electrodes were analyzed for their content, as also the fume that was collected from these welds. Table 6.2 compares the bulk fume compositions for the different welds – these results are from the chemical analysis of fume. Table 6.3 lists the results from surface analysis by XPS. As seen from tables 6.2 and 6.3, the composition of fume was quite similar when the same electrode was used, even though the base metals were different. The MS pipe contained no Cr, yet the GMAW of the MS pipe with a SS electrode produced fume with a high Cr content. This suggests that most fume evolved from the electrode, with almost no contribution from the base metal.

6.2 Metals and Chrome Analysis

GMAW fume samples were collected for elemental analysis and chrome analysis. The first part of the elemental analysis was carried out for metal content at the Trace Metal Lab at the Harvard School of Public Health. Table 6.4 lists the results of this analysis. Subsequently, surface analysis was performed using XPS at the Gordon-McKay Labs. Table 6.5 shows these results.

From table 6.4, one can see that the metal content in fume is reduced as compared to theoretical predictions. This is because of oxygen pickup. The surface analysis results in table 6.5 show high oxygen contents confirming that the metals have been oxidized following formation.

Fume samples were also analyzed for hexavalent chrome in addition to the total chromium content. NIOSH method 7600 was used for this purpose, though there is some uncertainty about this procedure (ref. 1). During the steps following digestion of the filters, one of the reagents could potentially oxidize the chrome species, thus all the Cr could be converted to Cr VI.

The results from this analysis are presented in figure 6.6. Cr VI was present in the fume in amounts ranging from 0.02 to 0.25 percent by weight of total fume, which correspond to 0.29 to 2.05 percent of the chrome content in fume. There is a difference in Cr VI content versus Cr (g) by three orders of magnitude between theoretical predictions during formation and experimental results. This suggests that other forms of chromium have indeed been oxidized to Cr VI following formation. The amount of Cr VI, however is still small when compared to total fume, or even total Cr in fume.

These experimental results are compared to literature values. Moreton, et. al, conducted fume emissions tests when welding stainless steels (ref. 34). The data for electrode type E316L from their report, which is most similar in composition to the electrode in this study, are compared to our numbers. This comparison is given in Table 4.7. For most metals, especially total Cr and Cr VI, there is substantial agreement with their numbers.

6.3 Other Discussion

Experimental results cannot be expressed in terms of $\mu\text{g}/\text{m}^3$ since a sampling time of 3 minutes is insufficient to correlate these numbers to meaningful time weighted averages that form the basis of OSHA and other mandates. There is no clear way of doing this.

The experiments performed under the inert gas conditions were not supposed to undergo any further reactions outside the arc-column (or electrode tip or weld-pool). The fume collected on the filter was expected to be the fume formed. However, as seen in tables 6.4 through 6.6, these samples were similar to those collected under regular conditions. This is because of leaks in the system that caused further oxidation of the particles after formation. In the future, the chamber will have to be made air-tight for these experiments.

7. Conclusions

1. Given the welding electrode and shielding gas compositions, it is possible to predict the welding fume composition during formation as generated by vaporization from the GMAW droplets of stainless steel, through thermodynamic calculations.
2. These calculations were applied to the study of chromium in welding fume generated by GMAW of SS.
3. The chromium content was found to vary with the shielding gas composition.
4. Cr (g) was the dominant form of the chromium in fume for all the shielding gas compositions.
5. Calculations showed the presence of Cr VI in the form of CrO₃ (g) in welding fume, although its vapor pressure was 2 to 4 orders of magnitude below Cr (g).
6. CrO₃ in the gas is much less than Cr (g), but Cr (g) may later oxidize in air.
7. The amount of CrO₃ (g) was also shown to vary with the oxidizing potential of the shielding gas, but by less than 1% for a 900% increase in oxygen content.
8. The study proved that the CrO₃ (g) that evolves from the droplet by vaporization is very small, but in the future it must be understood if it is later converted to a harmful form.
9. More tests need to be performed to complete the study of chromium in welding fume – its nature (soluble vs. insoluble) and interaction with biological pathways require more understanding.

10. Studies are currently underway at the Harvard School of Public Health, Boston, MA, to study the effect of GMAW of SS on the lungs of rats. These studies are concerned with the role of chromium and Cr VI.
11. The experiments also showed that the electrode is the main source of fume, with insignificant contributions from the base metal.
12. The theoretical method established in this work can be applied to study of other metal vapors, including manganese, in fume generated by GMAW of SS.
13. These concepts can be extended to FCAW and other joining processes that generate a considerable amount of fume.
14. A model needs to be established that will correlate predicted values during fume formation to those found by experimentation.

8. References

1. *Impact of Recent and Anticipated Changes in Airborne Emission Exposure Limits on Shipyard Workers*, Report prepared by the Navy Joining Center and Navy/Industry Task Group, NSRP, University of Michigan, March 1996.
2. W.S. Beckett: **Occupational and Environmental Respiratory Disease**, Harber, et al. (ed.), Mosby, New York, pp. 704-717.
3. G.J. Naherne: *Literature Review Update on Nickel Containing Welding Fume (1988 to mid-1994)*, Welding Institute of Canada Report RC512, 1995.
4. S. Sferlazza, and W. Beckett: *The Respiratory Health of Welders: State of the Art*, **Amer. Rev. Respir. Dis.**, 1991, Vol. 143, pp. 1134-1148.
5. J.J. Beumont and N. S. Weiss: *Lung Cancer Among Welders*, **Journal of Occupational Medicine**, December 1981, Vol. 23, pp. 839-844.
6. Gael Ulrich, Chem. Eng., University of New Hampshire, Durham, NH: *Progress Report: Welding Fume: Emissions and Properties*, Prepared for Edison Welding Institute, Columbus, OH, March 25, 1996.
7. Michael Aschner, and Judy L. Aschner: *Manganese Transport Across the Blood-Brain Barrier: Relationship to Iron Homeostasis*, **Brain Research Bulletin**, June 1990, Vol. 24, pp. 857-860.
8. Sidney A. Katz, Harry Salem: *The Toxicology of Chromium with respect to its Chemical Speciation: A Review*, **Journal of Applied Toxicology**, 1993, Vol. 13(3), pp. 217-224.
9. Mitchell D. Cohen, Biserka Kargachin, Catherine B Klein, and Max Costa: *Mechanisms of Chromium Carcinogenicity and Toxicity*, **Critical Reviews in Toxicology**, 1993, Vol. 23(3), pp. 255-281.
10. ASM, **Metals Handbook**.
11. S. Kimura, M. Kobayashi, T. Godai, and S. Minato: *Investigations on Chromium in Stainless Steel Welding Fumes*, **Welding Journal**, July 1979, pp. 195s-204s.
12. R.F. Heile and D.C. Hill: *Particulate Fume Generation in Arc Welding Processes*, **Welding Journal**, July 1975, Vol. 54, pp. 201s-210s.

13. C.N. Gray, P.J. Hewitt, and R. Hicks: *The effect of Oxygen on the rate of fume formation in metal inert gas welding arcs*, **Weld Pool Chemistry and Metallurgy**, an International Conference, 1980, Paper 27, pp. 167-176.
14. Heidi Gibson: **Influence of Shielding Gas Composition on Alloy Recovery during Gas Metal Arc Welding**, Masters Thesis, MIT, June 1993.
15. A. Block-Bolten and T.W. Eagar: *Selective Evaporation of Metals from Weld Pools*, **Trends in Welding Research in the United States**, S.A. David (ed.), ASM, Menlo Park, OH, 1982, pp. 53-73.
16. F.Y. Speight, editor: **Fumes and Gases in the Welding Environment**, American Welding Society, Miami, FL, 1979.
17. J.R. Antonini, et al.: *Pneumotoxicity and Pulmonary Clearance of Different Welding Fumes after Intratracheal Instillation in the Rat*, **Toxicology and Applied Pharmacology**, 1996, Vol. 140, pp. 188-199.
18. C.N. Gray, P.J. Hewitt, and P.R.M. Dare: *New approach would help control weld fumes at source, part two: MIG Fumes*, **Welding and Metal Fabrication**, October 1982, pp. 393-397.
19. Harvey R. Castner: *Gas Metal Arc Welding Fume Generation Using Pulsed Current*, **Welding Journal**, February 1995, Vol. 74, pp. 59s-68s.
20. V. Voitkevich: **Welding Fumes: Formation, Properties, and Biological Effects**, Abington Publishing, Cambridge, U.K., 1995.
21. D.C. Willingham, and D.E. Hilton: *Some Aspects of Fume Emissions from MIG Welding Stainless Steel*, **Welding and Metal Fabrication**, July 1986, pp. 226-229.
22. O. Grong and N. Christensen: *Factors Controlling MIG Weld Metal Chemistry*, **Scandinavian Journal of Metallurgy**, 4 (1983), pp. 155-165.
23. N. Meyendorf: *Metal Gas Reactions in Gas-Shielded Arc Welding*, **Welding International**, 1988, No. 7, pp. 653-657.
24. A. Block-Bolten and T.W. Eagar: *Metal Vaporization from Weld Pools*, **Metallurgical Transactions**, September 1984, Vol. 15B, pp. 461-469.
25. Larry A. Jones: **Dynamic Electrode Forces in Gas Metal Arc Welding**, Doctoral thesis, MIT, February 1996.

26. Gedeon, S., and Rudd, S.J.: *The Effect of Shielding Gas Composition on Mild Steel GMA Weld Composition, Properties, and Porosity*, WIC Final Report RC422/91, January 1992.
27. J.F. Lancaster (ed.): **The Physics of Welding**, Pergamon Press, Oxford, UK, 1984.
28. R.E. Francis, J.E. Jones, and D.L. Olson: *Effects of Gas Oxygen Activity on Weld Metal Microstructure on GMA Welded Microalloyed HSLA Steel*, **Welding Journal**, Nov. 1990, pp. 408s-415s.
29. Robert V. Albert: **Fume Generation in Gas Metal Arc Welding**, Ph.D. thesis, University of New Hampshire, Durham, 1996.
30. E.A. Gulbransen, and S.A. Jansson: **Oxidation of Metals and Alloys**, ASM, Menlo Park, OH, 1971, pp. 63-86.
31. Ralph Hultgren, Raymond L. Orr, Philip D. Anderson, Kenneth K. Kelley: **Selected values of Thermodynamic Properties of Metals and Alloys**, John Wiley and Sons, Inc., New York, 1963.
32. Gael Ulrich, Chem. Eng., University of New Hampshire, Durham, NH: *Progress Report: Welding Fume: Emissions and Properties*, Prepared for Edison Welding Institute, Columbus, OH, February 2, 1995.
33. *Laboratory Method for Measuring Fume Generation Rates and Total Fume Emission of Welding and Allied Processes*, American Welding Society, Miami, FL, 1992. (Document no. ANSI/AWS F.1-2-92).
34. J. Moreton, E. A. Smars, K. R. Spiller: *Fume emission when welding stainless steel*, **Metal Construction**, 1985, 17 (12), 794-798.

Analysis	Fe	C	Cr	Cu	Mn	Mo	Ni	P	S	Si
Manufacturer specs. *	67.26	0.04	20.50	<0.01	1.90	<0.01	9.80	0.023	0.006	0.45
Recent analysis **	66.9	0.058	20.8	-	1.77	0.046	9.75	-	-	0.56

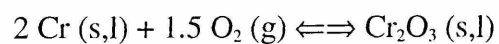
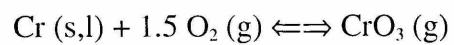
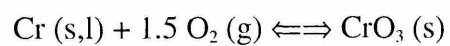
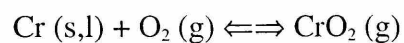
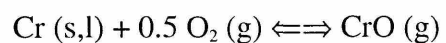
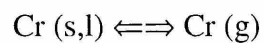
Values given in weight percent

* Specifications for McKay 308 SS electrode, from Hobart Brothers, Troy, OH

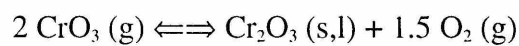
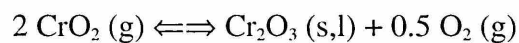
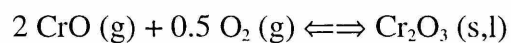
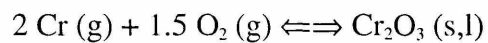
** Elemental Analysis by Luvak Inc. (see section 5.4.1)

Table 4.1 Composition of type 308 Stainless Steel

Equilibrium over Cr (s,l)



Equilibrium over Cr₂O₃ (s,l)



CrO₂ (g) and CrO₃ (s) are unstable over 800 K

Table 4.2 Chemical Equilibrium in the Cr-O system

Element	C	Cr	Cu	Fe	Mn	Ni
Activity	0.00134	0.315	0.00048	0.753	0.0247	0.0614
Temperature (in K)	1800	1628	1823	1628	1863	1873

Activities obtained from Hultgren's tables (ref. 31) (See section 4.0)

Table 4.3 Activities of Selected Components of Type 308 Electrodes

Shielding Gas	Cr	Cu	Fe	Mn	Ni
99 Ar 1 O2	24.52	0.0216	52.51	14.89	5.99
98 Ar 2 O2	24.33	0.0245	52.75	14.74	6.09
95 Ar 5 O2	23.77	0.0257	53.45	14.29	6.41
90 Ar 10 O2	22.80	0.0281	54.56	13.52	7.04
95 Ar 5 CO2	26.88	0.0578	58.73	6.26	5.99

(Weight Percentage of Total Vapor)

Total Vapor = Gases in Appendix A - (Ar (g), O (g), O₂ (g), O₃ (g), CO (g), CO₂ (g))

GMAW using 308 SS electrodes, droplet temperature = 2400° C

Table 4.4 Theoretical Predictions of Metal Content in Vapor

Shielding Gas	Cr (g)	CrO (g)	CrO ₂ (g)	CrO ₃ (g)
99 Ar 1 O ₂	19.86	5.76	4.14E-1	1.29E-4
98 Ar 2 O ₂	19.69	5.73	4.13E-1	1.29E-4
95 Ar 5 O ₂	19.19	5.65	4.11E-1	1.30E-4
90 Ar 10 O ₂	18.35	5.50	4.07E-1	1.31E-4
95 Ar 5 CO ₂	22.05	5.99	4.02E-1	1.17E-4

(Weight Percentage of Total Vapor)

Total Vapor = Gases in Appendix A - (Ar (g), O (g), O₂ (g), O₃ (g), CO (g), CO₂ (g))

Shielding Gas	Cr (g)	CrO (g)	CrO ₂ (g)	CrO ₃ (g)
99 Ar 1 O ₂	76.27	22.14	1.59	4.96E-4
98 Ar 2 O ₂	76.21	22.19	1.60	5.00E-4
95 Ar 5 O ₂	76.01	22.36	1.63	5.14E-4
90 Ar 10 O ₂	75.66	22.66	1.68	5.40E-4
95 Ar 5 CO ₂	77.54	21.05	1.42	4.12E-4

(Weight Percentage of Total Chrome Vapor)

Total Chrome vapor = Column 2 in table 4.4

GMAW using 308 SS electrodes, droplet temperature = 2400° C

Table 4.5 Theoretical Calculations for Chrome Species in Vapor

	Analysis	Fe	C	Cr	Cu	Mn	Mo	Ni	P	S	Si
SS Electrode Type 308	Manu. specs. *	67.26	0.04	20.50	<0.01	1.90	<0.01	9.80	0.023	0.006	0.45
SS Electrode Type 308	Recent analysis **	66.9	0.058	20.8	-	1.77	0.046	9.75	-	-	0.56
MS Electrode ER70S-3	Manu. Specs. ***	97.89	0.07	0.03	0.11	1.23	0.01	0.05	0.011	0.011	0.59
MS Electrode ER70S-3	Recent analysis **	97.9	0.096	0.046	0.16	1.16	0.005	0.038	-	-	0.55
SS Pipe 304L/304	Manu. Specs. #	70.40	0.02	18.31	0.36	1.77	0.30	8.21	0.031	0.015	0.32
MS Pipe A 500	Manu. Specs. ##	98.61	0.19	0	0.028	0.81	-	0	0.014	0.007	-

Values given in weight percent

* Specifications for McKay 308 SS electrode, from Hobart Brothers, Troy, OH
 ** Elemental Analysis by Luvak Inc. (see section 5.4.1)
 *** Specifications for Hobart ER70S-3 electrode, from Hobart Brothers, Troy, OH
 # Specifications for 304L/394 pipe from Stainless Pipe and Fittings, Randolph, MA
 ## Specifications for A 500 pipe from Novel Iron Works, Greenland, NH

Table 6.1 Elemental Compositions of Electrodes and Pipes

Base Metal	Electrode	Co	Cr	Cu	Fe	Mn	Mo	Ni
SS	SS	0.015	12.99	0.213	15.8	15.34	0.023	1.335
SS	MS	0.011	0.2	0.914	35.2	9.76	0.009	-
MS	SS	0.018	13.08	0.175	17.7	11.85	0.019	2.507
MS	MS	0.19	0.52	0.845	37.8	8.8	0.013	-

GMAW of 308 SS, 30V, 300 ipm, 98 Ar - 2 O₂ Shielding gas

Analysis performed at the Trace Metals Lab, Harvard School of Public Health, Boston, MA

Table 6.2 Chemical Analysis of MS and SS Fume

Base Metal	Electrode	Cr	Fe	Mn	Si	O	C
SS	SS	4.17	7.12	4.93	-	57.85	25.93
SS	MS	-	10.12	3.37	-	58.16	28.36
MS	SS	3.46	6.24	3.99	4.17	55.40	26.74
MS	MS	-	9.93	2.98	3.71	55.67	27.71

GMAW of 308 SS, 30V, 300 ipm, 98 Ar - 2 O₂ Shielding gas

Table 6.3 Surface Analysis of MS and SS Fume
by X-ray Photo-electron Spectroscopy (XPS)

Shielding Gas	Chamber	Co	Cr	Cu	Fe	Mn	Mo	Ni
Ar	Room air	0.022	12.31	0.198	26.5	10.88	0.032	3.528
Ar	Inert gas	0.04	8.95	0.162	39.2	7.58	0.073	3.645
98 Ar, 2 O ₂	Room air	0.015	12.99	0.213	15.8	15.34	0.023	1.335
98 Ar, 2 O ₂	Inert gas	0.018	12.46	0.241	21.00	17.43	0.024	1.045
95 Ar, 5 O ₂	Room air	0.02	10.99	0.208	48.1	13.53	0.013	1.238
95 Ar, 5 O ₂	Inert gas	0.014	10.24	0.182	15.2	12.78	0.006	1.062
95 Ar, 5 CO ₂	Room air	0.016	11.87	0.193	23.7	11.63	0.047	2.182
95 Ar, 5 CO ₂	Inert gas	0.015	11.09	0.201	18.5	12.67	0.016	1.517
100 CO ₂	Room air	0.015	6.92	0.214	25.3	8.96	0.03	3.263
100 CO ₂	Inert gas	0.015	14.55	0.178	28.9	8.36	0.02	2.261

GMAW using 308 SS, 30V, 300 ipm

Table 6.4 Chemical Analysis of Fume Samples
For Metals Only

Shielding Gas	Chamber	Cr	Fe	Mn	Si	O	C
Ar	Room air	3.27	6.17	5.57	4.37	56.37	24.25
Ar	Inert gas	2.11	7.77	4.32	3.90	56.86	25.04
98 Ar, 2 O ₂	Room air	4.17	7.12	4.93	-	57.85	25.93
98 Ar, 2 O ₂	Inert gas	3.16	5.85	4.79	3.86	53.53	28.82
95 Ar, 5 O ₂ *	Room air	4.40	7.83	3.47	-	61.48	22.82
95 Ar, 5 O ₂	Inert gas	3.44	5.52	4.75	4.13	53.96	28.20
95 Ar, 5 CO ₂	Room air	3.32	6.61	4.78	2.60	56.60	26.08
95 Ar, 5 CO ₂	Inert gas	3.21	6.01	4.83	3.41	54.74	27.80
100 CO ₂	Room air	2.70	6.43	4.06	5.85	57.80	23.14
100 CO ₂	Inert gas	3.49	5.81	2.63	7.05	54.80	26.22

*Sample for 95%Ar, 5% O₂, Inert gas, not same run as samples for other analyses

Table 6.5 Surface Analysis of Fume Samples by X-ray Photo-electron Spectroscopy (XPS)

Shielding Gas	Chamber	Cr VI Percent of total fume Experiment*	Cr VI Percent of total fume Theory**	Cr VI Percent of total chrome Experiment*	Cr VI Percent of total fume Theory**
Ar	Room air	0.252		2.05	
Ar	Inert gas	0.101	0.0	1.13	0.0
98 Ar, 2 O ₂	Room air	0.199		1.53	
98 Ar, 2 O ₂	Inert gas	0.236	1.29E-4	1.89	5.00E-4
95 Ar, 5 O ₂	Room air	0.219		2.00	
95 Ar, 5 O ₂	Inert gas	0.155	1.30E-4	1.52	5.14E-4
95 Ar, 5 CO ₂	Room air	0.196		1.62	
95 Ar, 5 CO ₂	Inert gas	0.144	1.17E-4	1.30	4.12E-4
100 CO ₂	Room air	0.020		0.29	
100 CO ₂	Inert gas	0.152	-	1.05	-

Cr VI content reported as weight percentages

*Analysis of fume by NIOSH 7600 at DataChem Labs, Salt Lake City, UT

**From table 4.5

Table 6.6 Chrome Analysis Results

Sample	Co	Cr	Cr VI	Cu	Fe	Mn	Mo	Ni
Results from current study	0.015	12.99	0.199	0.213	15.8	15.34	0.023	1.335
Literature values (ref. 34) *	-	9.82 - 13.2	0.2 - 0.4	0.1 - 0.3	26.4 - 35.0	8.3 - 21.2	0.1 - 0.6	3.1 - 6.1

Shielding gas composition of 98% argon, 2% oxygen

*From ref. 34 for ER316LSi electrodes

Table 6.7 Comparison of Results with Literature

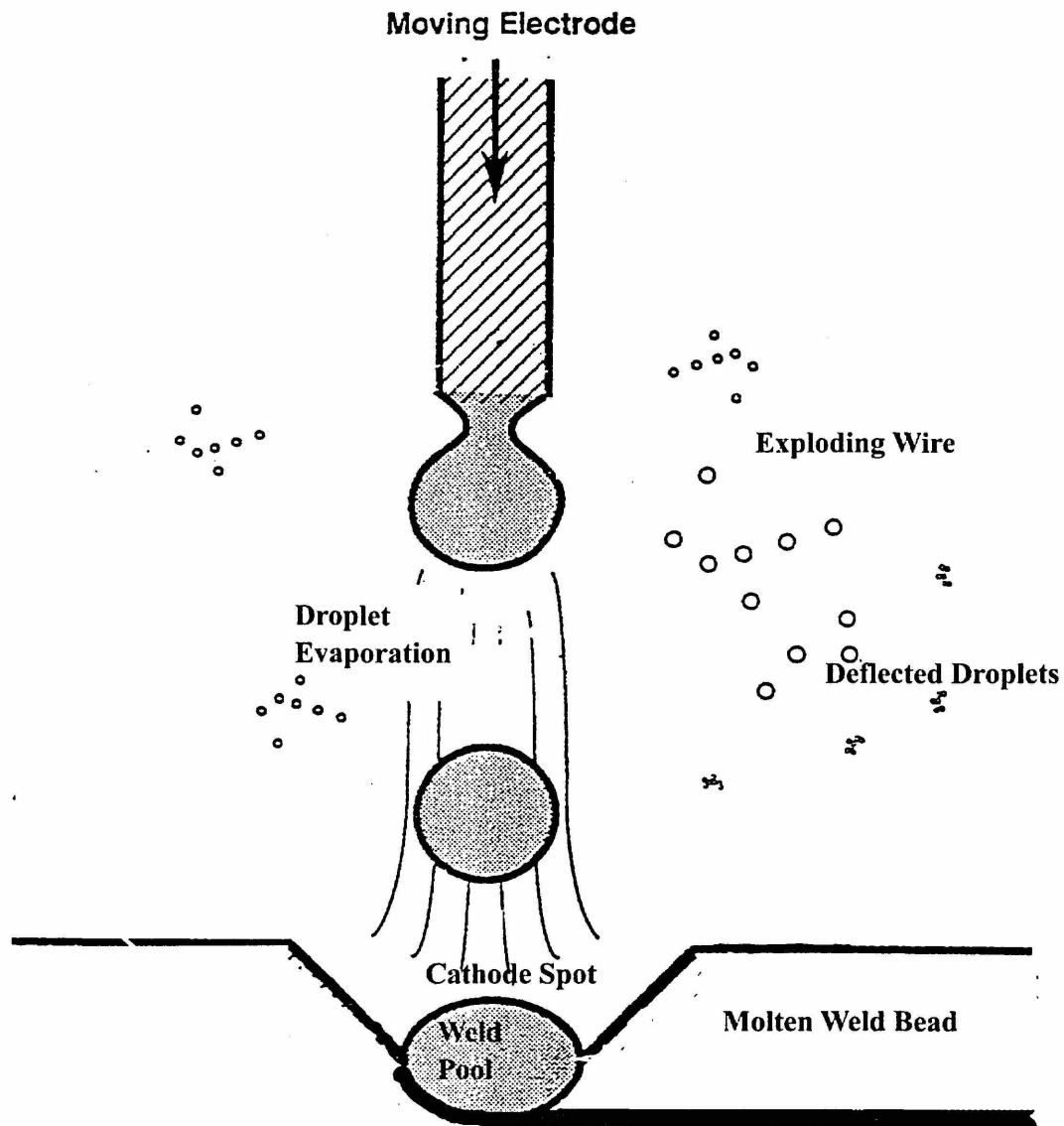


Figure 2.1 Fume Formation Model for GMAW

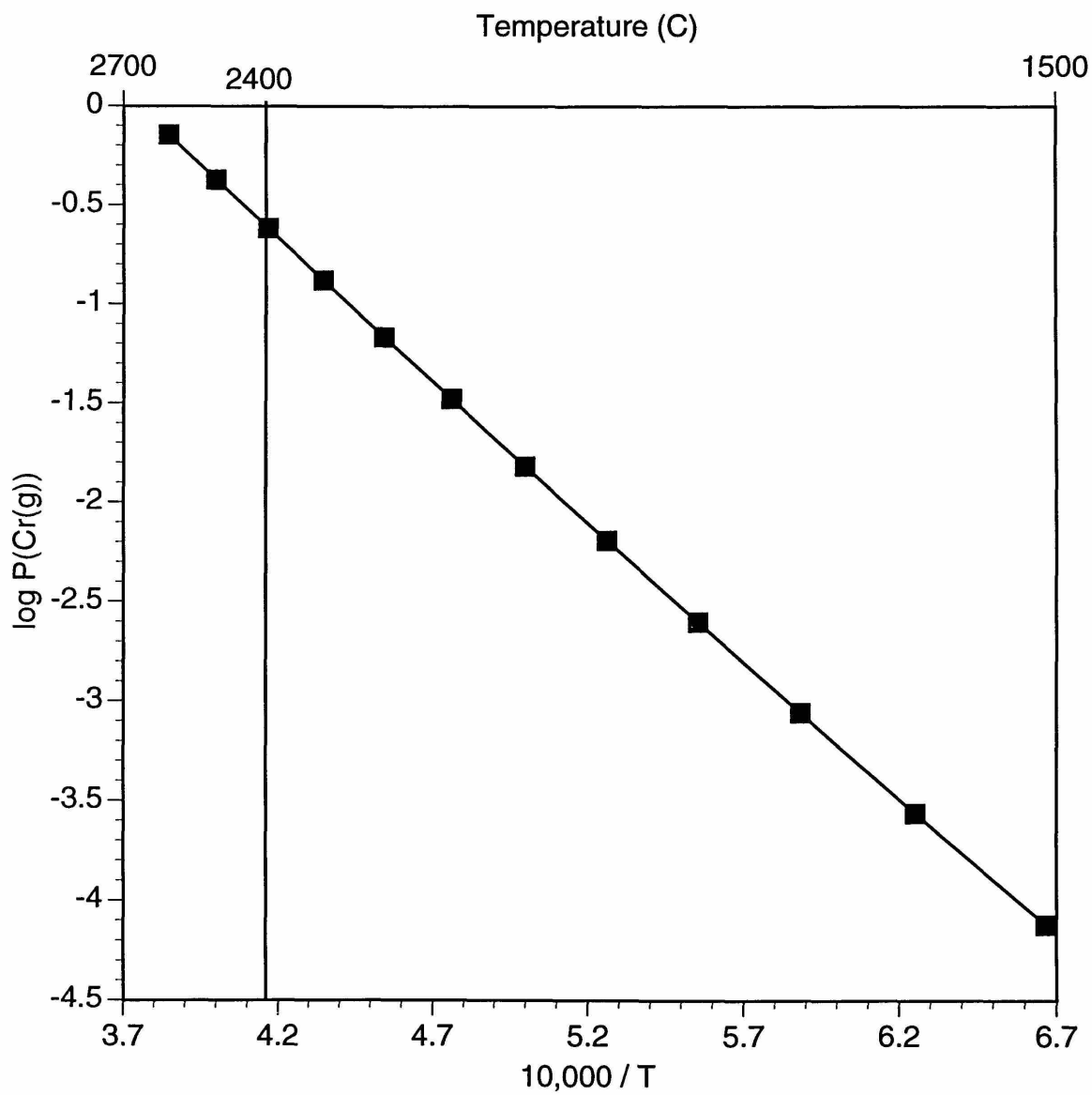


Figure 4.1 Vapor Pressure for Cr (g)

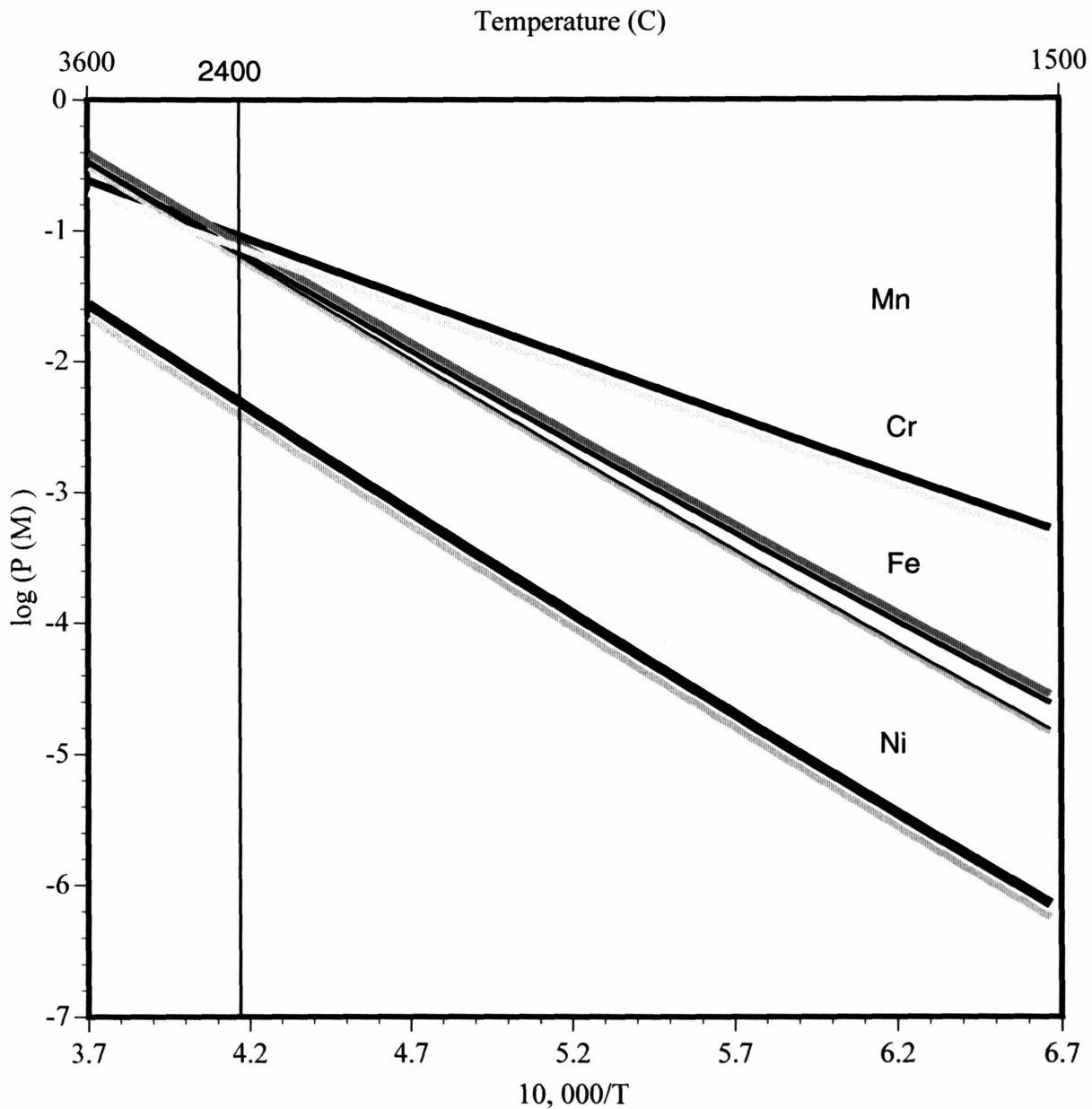


Figure 4.2 Partial Pressures for Alloying Elements in Stainless Steels

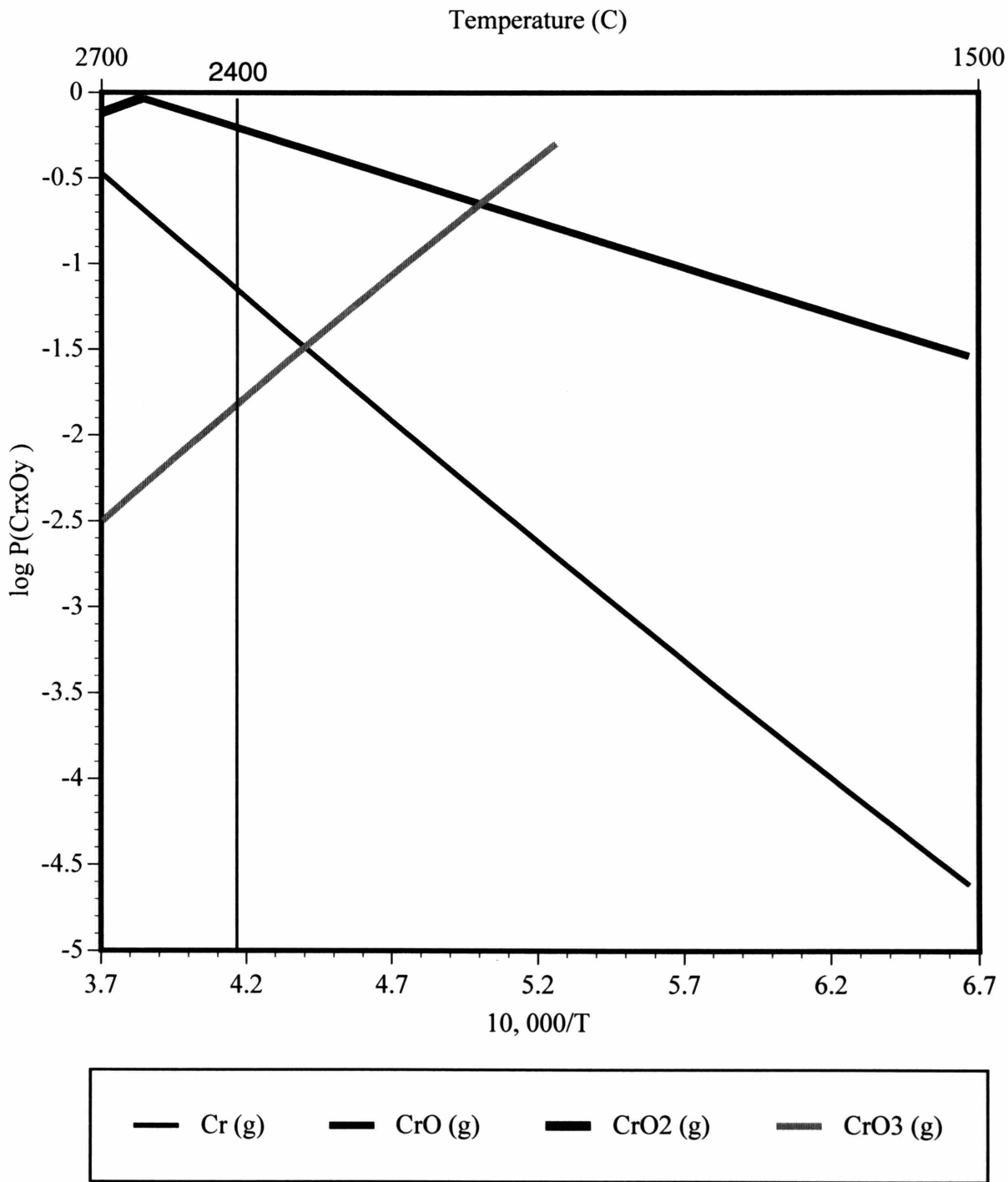


Figure 4.3 Chrome Species Vapor Pressures for 99% Argon, 1% O₂ Shielding Gas

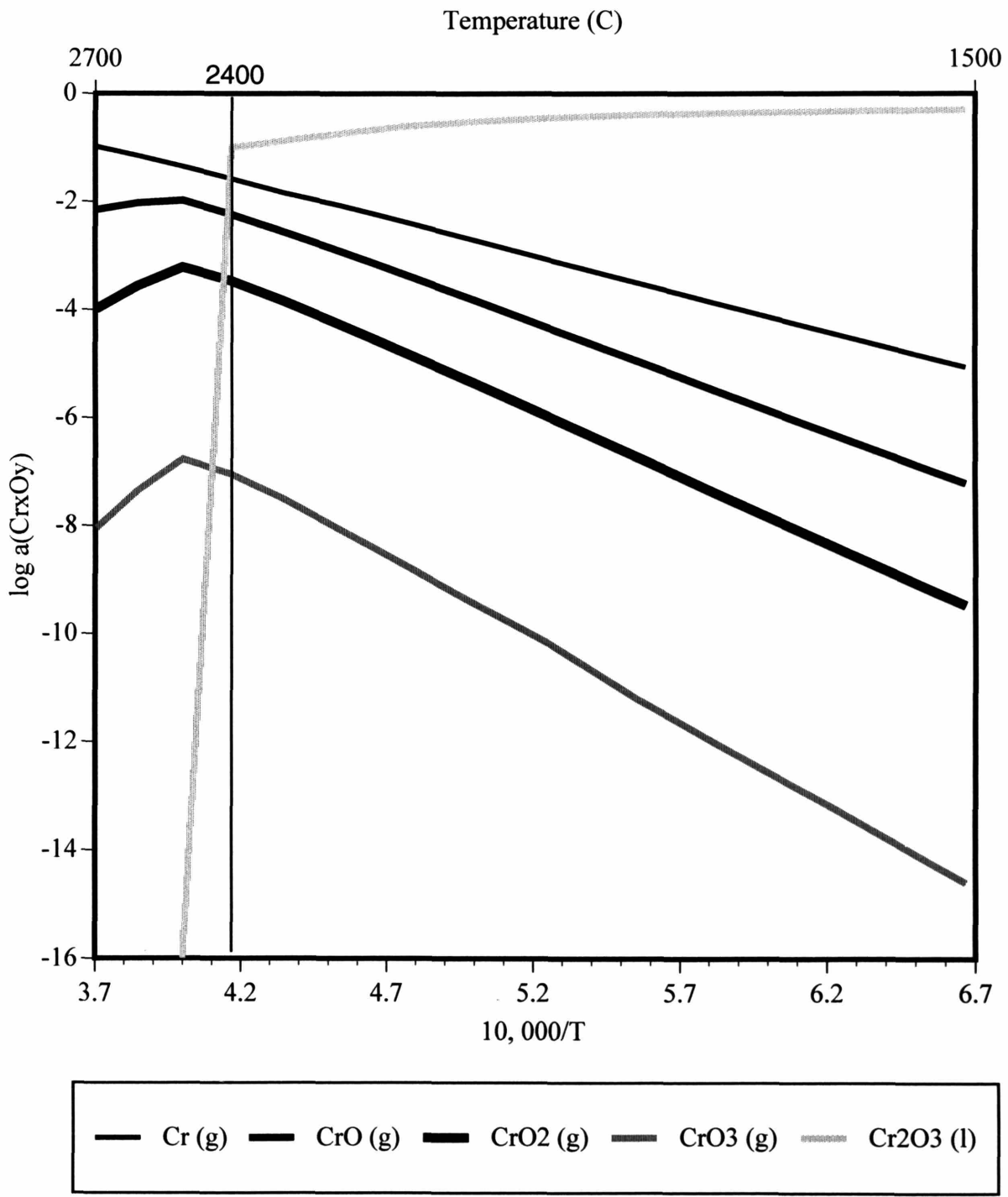


Figure 4.4 Chrome Species Activities (Vapor Pressures for gases) for 99% Argon, 1% O₂ Shielding Gas

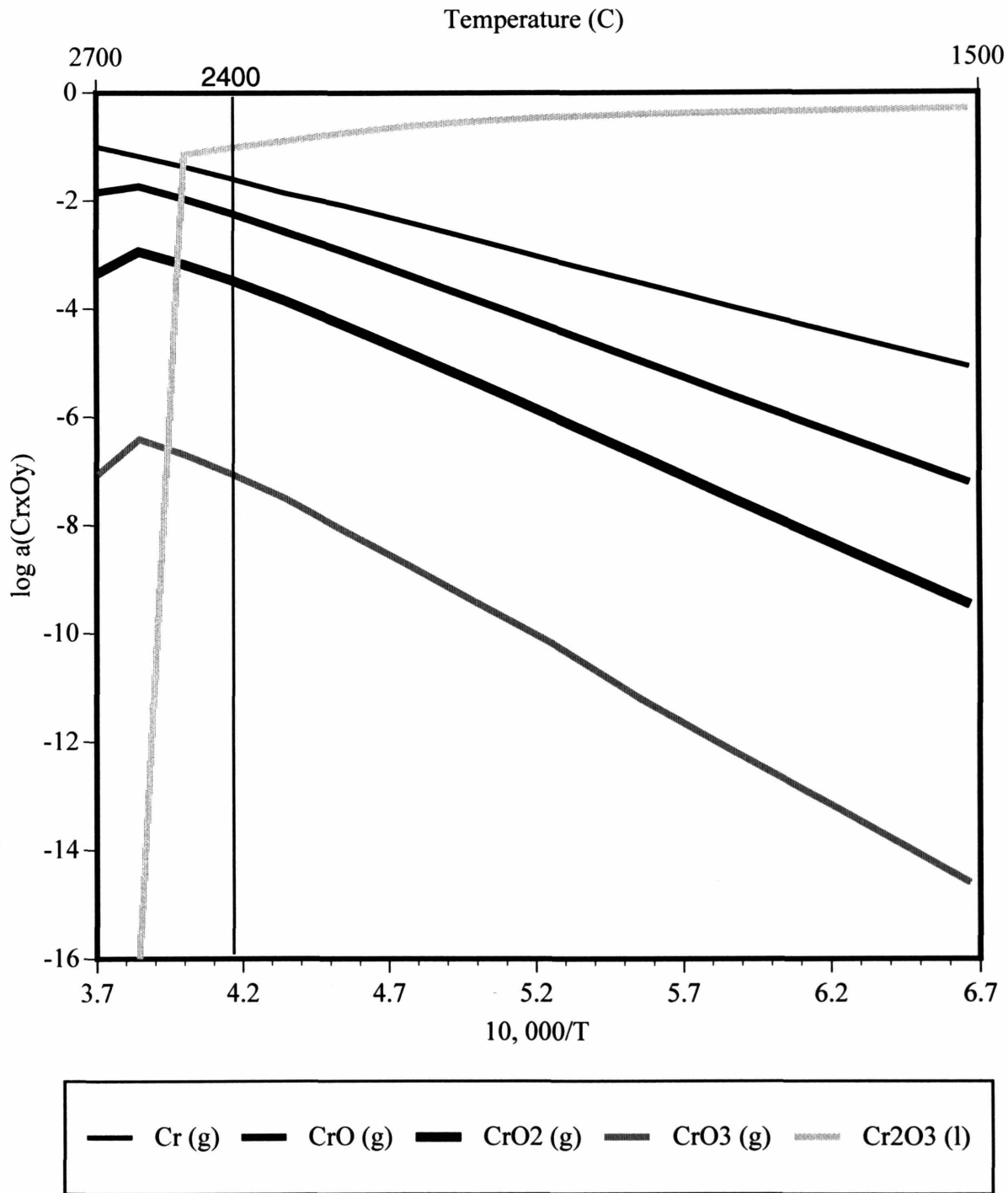


Figure 4.5 Chrome Species Activities (Vapor Pressures for gases) for 98% Argon, 2% O₂ Shielding Gas

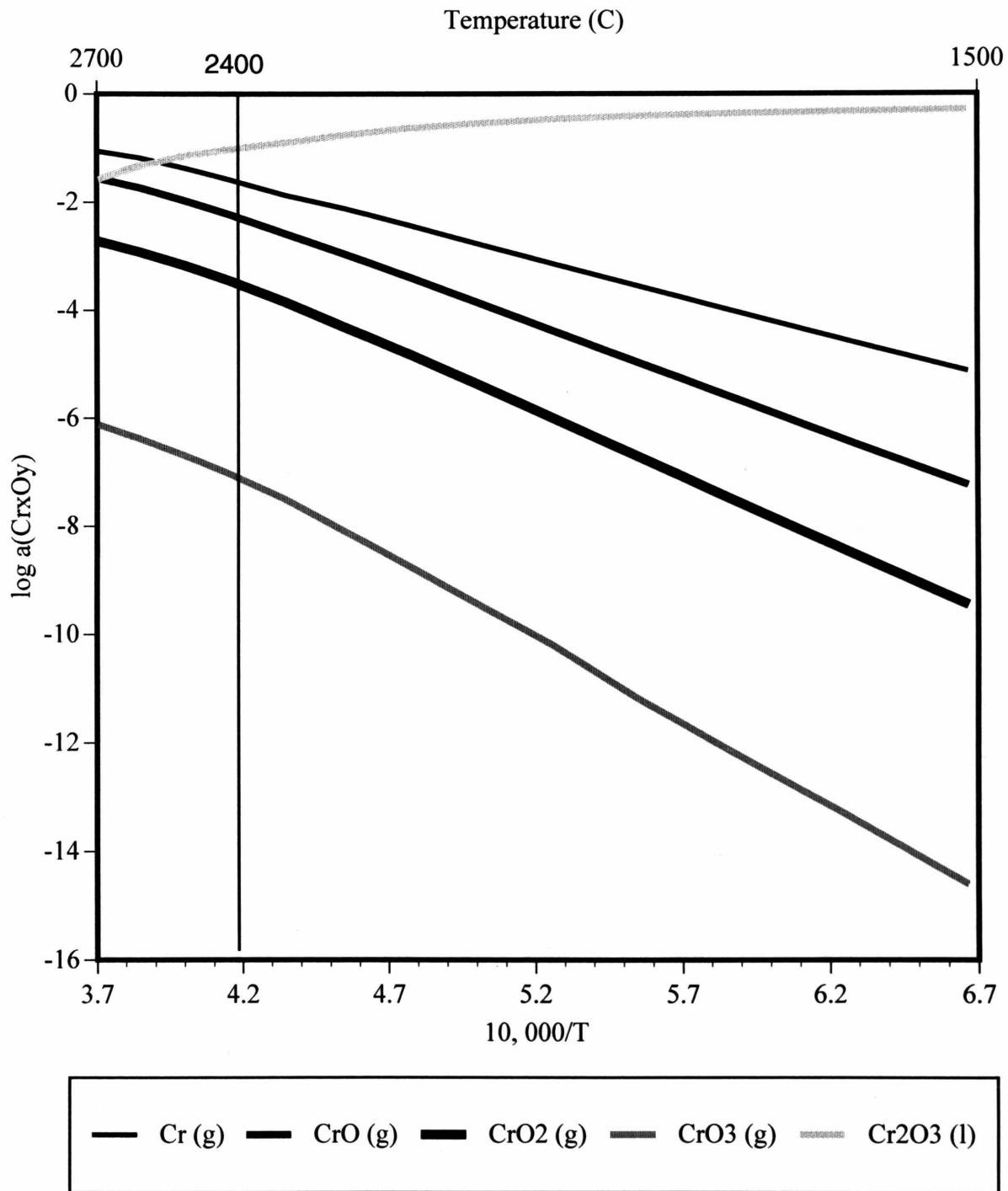


Figure 4.6 Chrome Species Activities (Vapor Pressures for gases) for 95% Argon, 5% O₂ Shielding Gas

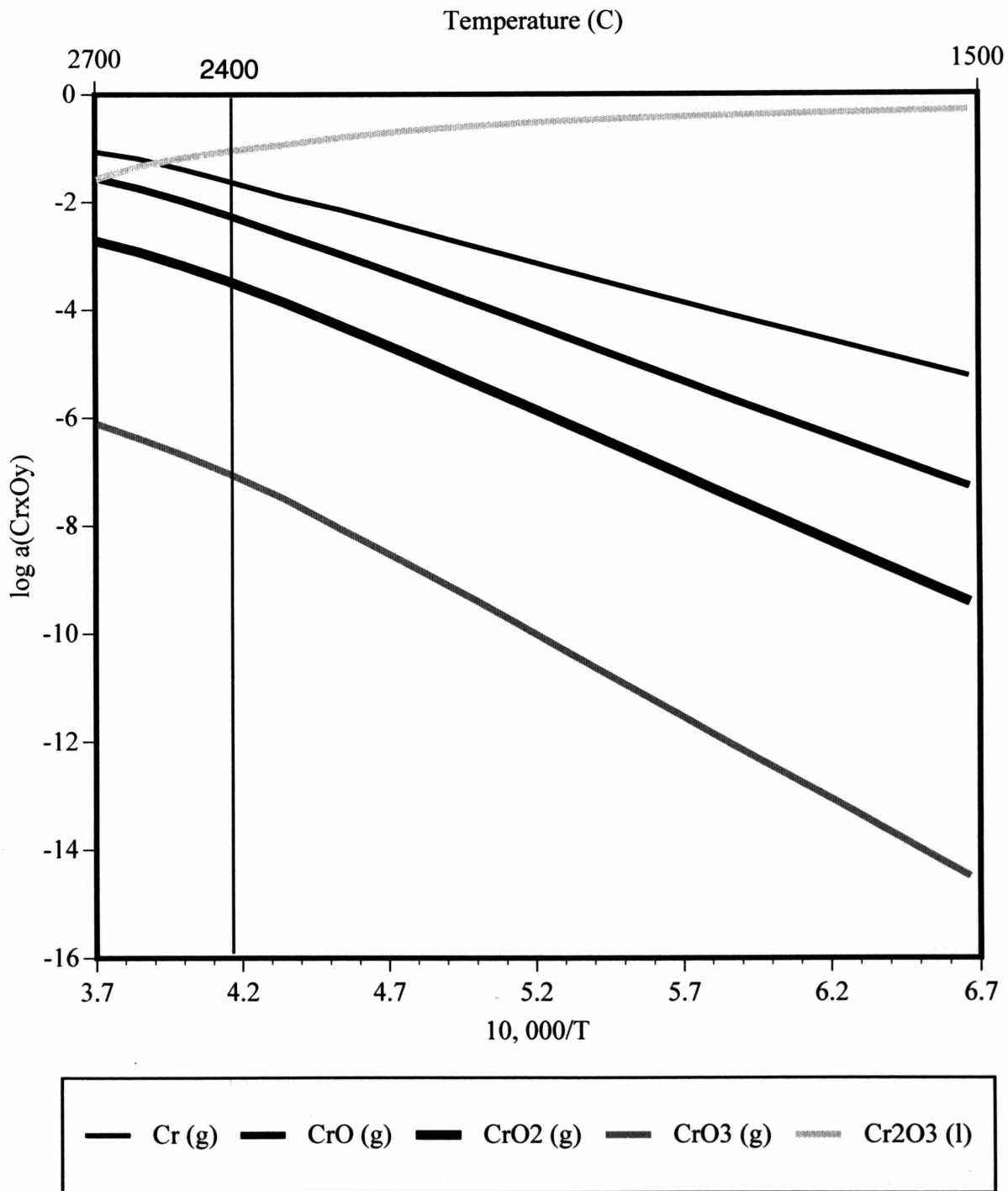


Figure 4.7 Chrome Species Activities (Vapor Pressures for gases) for 90% Argon, 10% O₂ Shielding Gas

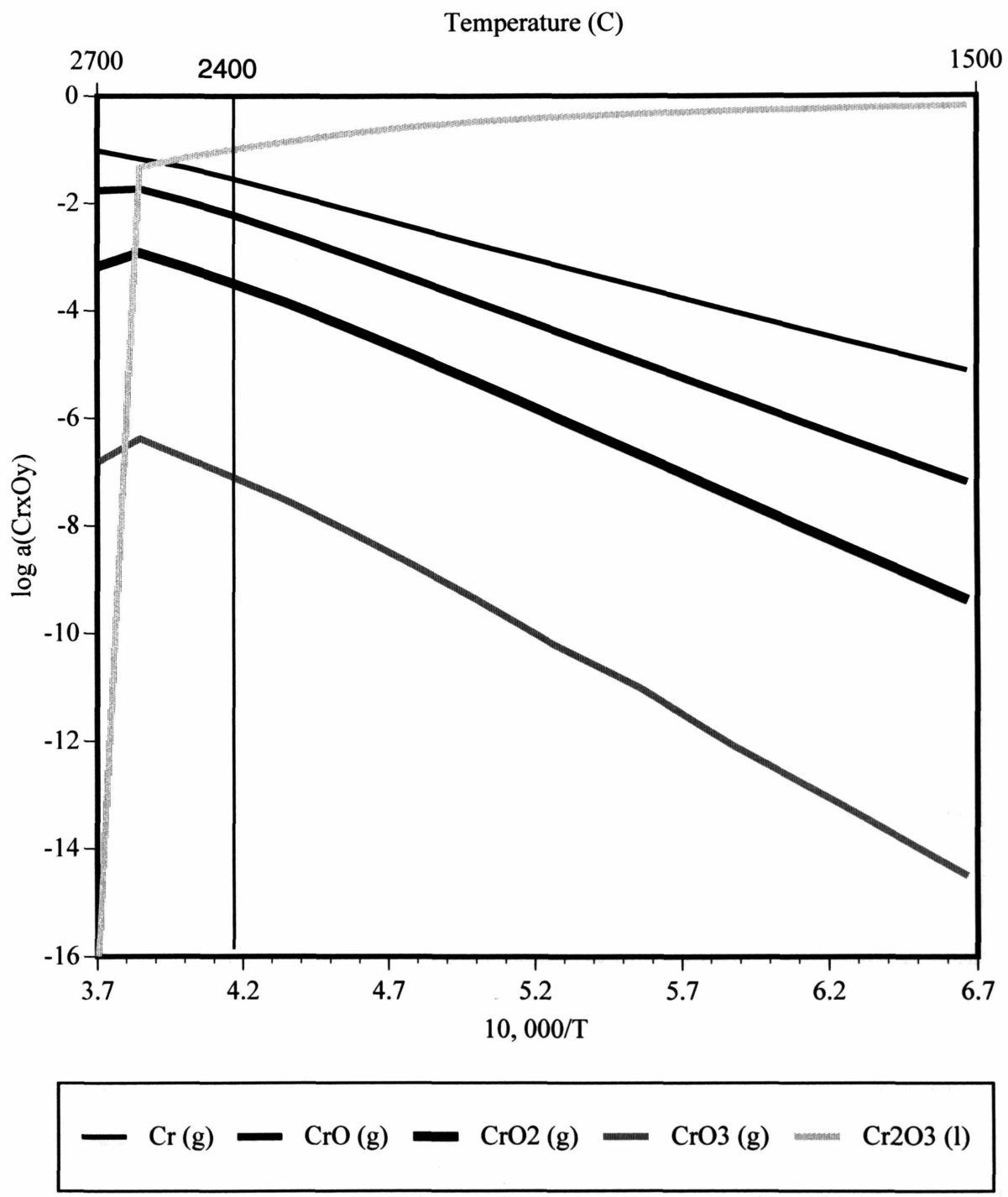


Figure 4.8 Chrome Species Activities (Vapor Pressures for gases) for 95% Argon, 5% CO₂ Shielding Gas

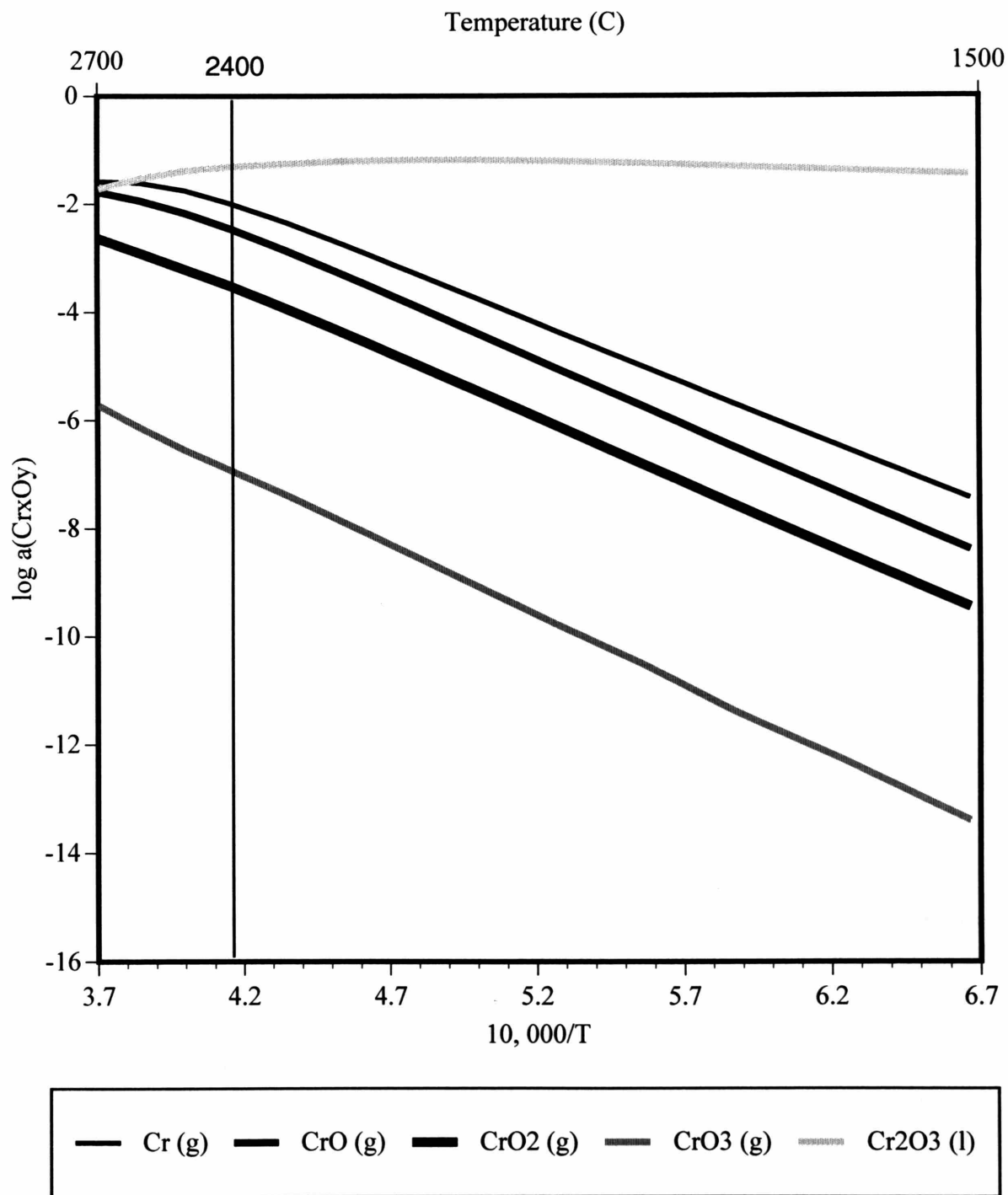


Figure 4.9 Chrome Species Activities (Vapor Pressures for gases) for 100% CO₂ Shielding Gas

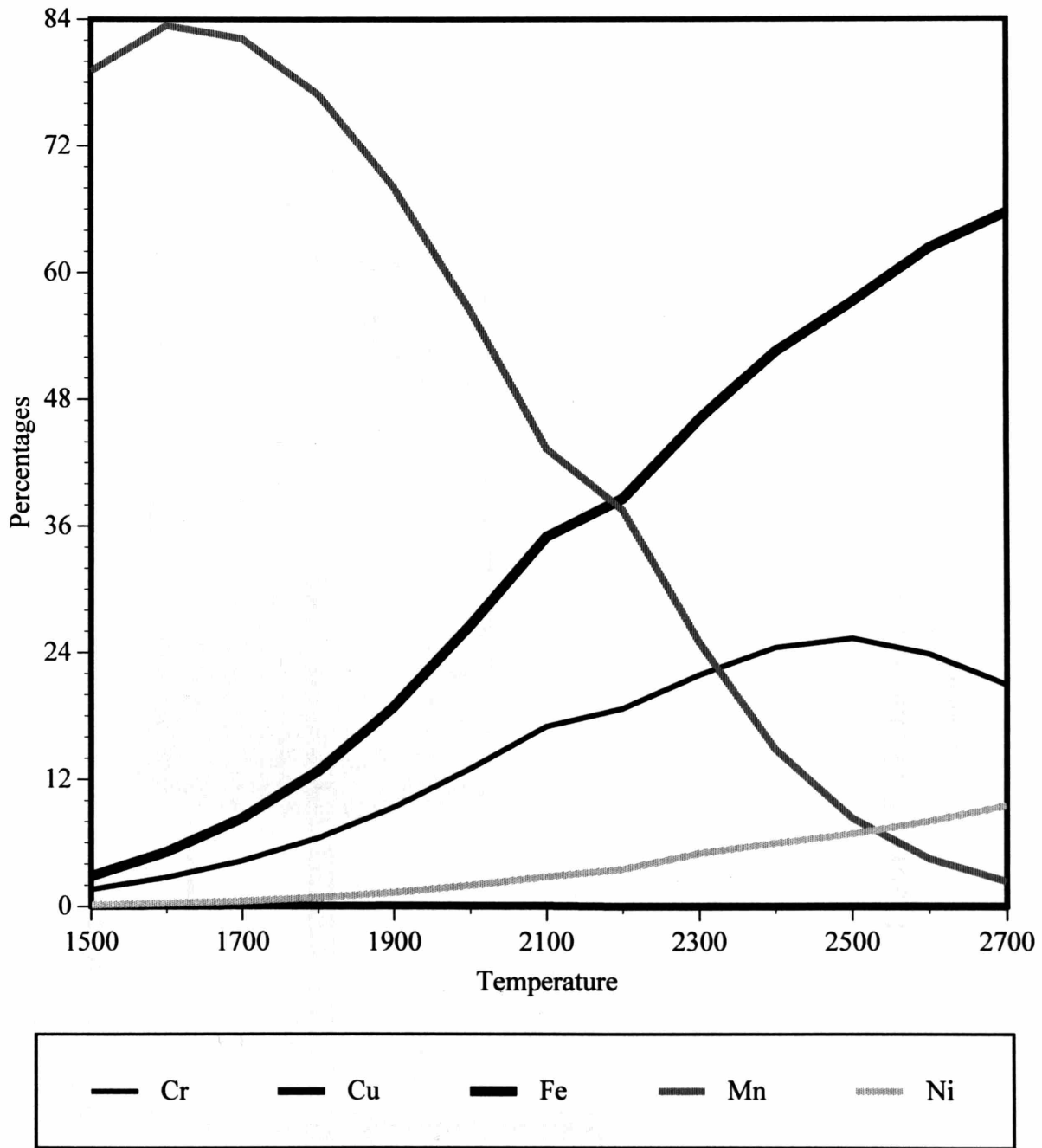


Figure 4.10 Metal Percentages in Vapor for 99% Argon, 1% O₂ Shielding Gas

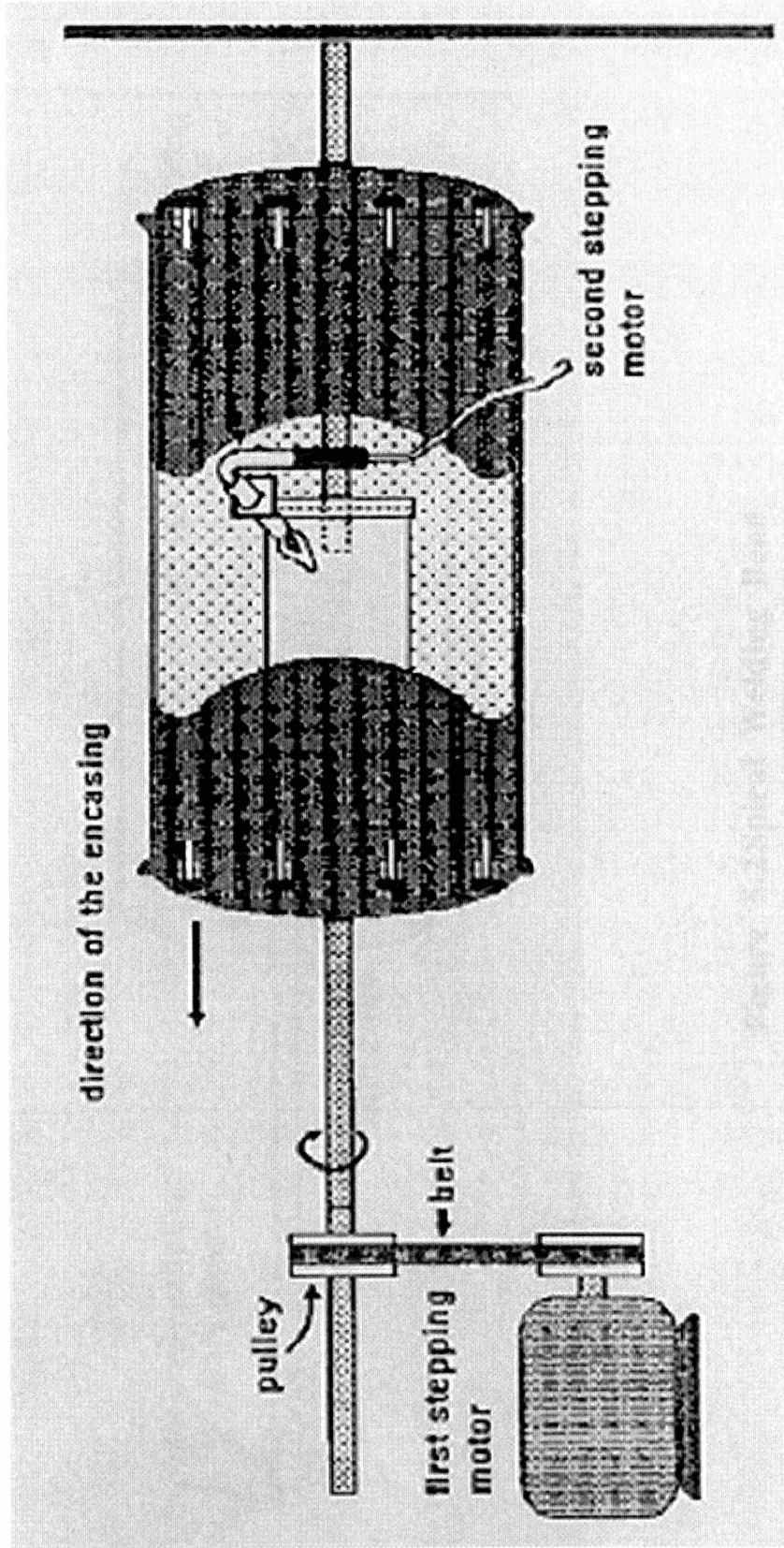


Figure 5.1 Fume Chamber Setup

(from ref. 32)

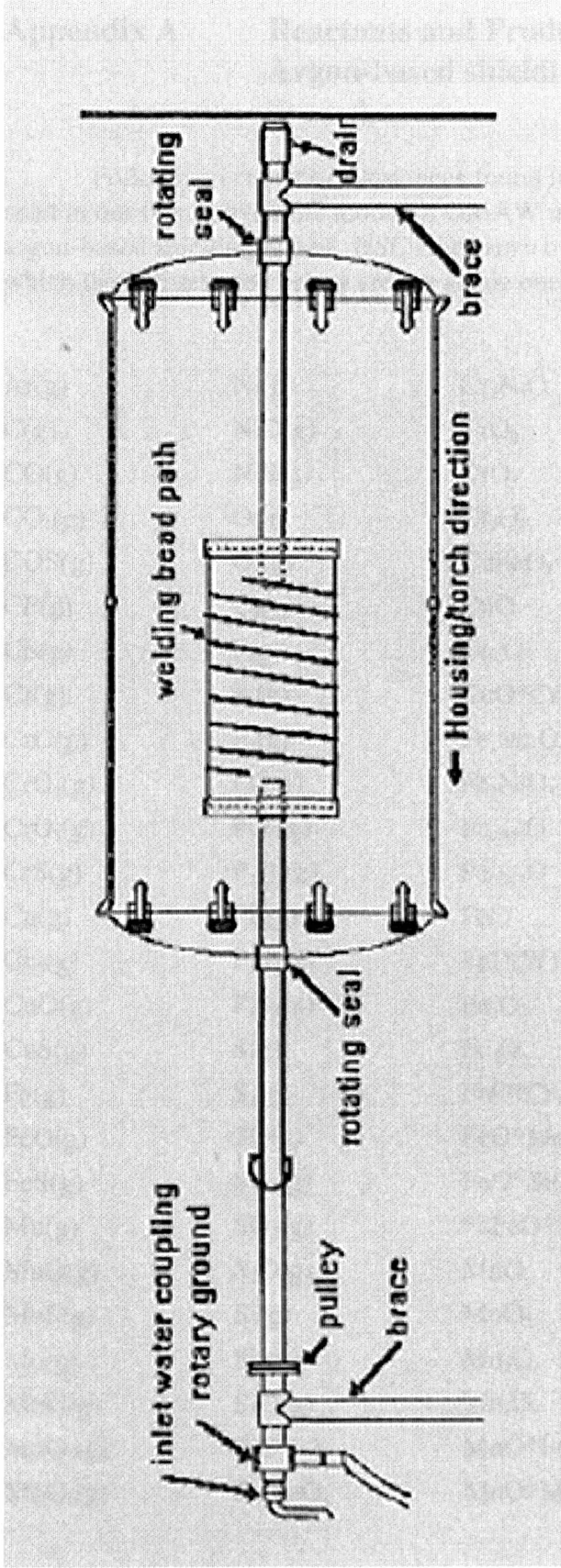


Figure 5.2 Spiral Welding Bead

(from ref. 32)

Appendix A Reactants and Products in GMAW using 308 SS and Argon-based shielding gases

Following is a list of substances found in the molten metal - shielding gas system used in our thermodynamic model of GMAW using a 308 stainless steel electrode and argon-based shielding gases. *HSC Chemistry* by Outokumpu lists 261 total species, of which the 126 selected below are the stable ones:

Ar(g)	Ni(g)	Cr ₂ NiO ₄	MnO*SiO ₂	C(D)
C(g)	NiO(g)	CrO ₂	*2MnO*SiO ₂	Cr(l)
CO(g)	NiS(g)	CrO ₃	MoO ₂	Cr
CO ₂ (g)	O(g)	Cr ₂ O ₃	MoO _{2.75}	CrSi
COS(g)	O ₂ (g)	CuFeO ₂	MoO _{2.87}	Cu
CP(g)	O ₃ (g)	CuO	MoO _{2.88}	Fe
CS(g)	P(g)	Cu ₂ O	MoO ₃	Fe ₃ Mo ₂
Cr(g)	P ₂ (g)	CuO*Cr ₂ O ₃	NiO	FeSi
CrO(g)	P ₃ (g)	Fe ₂ MnO ₄	NiO*Cr ₂ O ₃	Fe ₃ Si
CrO ₂ (g)	PO(g)	Fe ₂ NiO ₄	NiO*Fe ₂ O ₃	Mn
CrO ₃ (g)	PO ₂ (g)	Fe _{0.945} O	P ₂ O ₃	MnSi
CrS(g)	P ₂ O ₃ (g)	Fe _{0.947} O	SiO ₂	Mo
Cu(g)	PS(g)	FeO	SiO ₂ (l)	Ni
Cu ₂ (g)	P ₄ S ₄ (g)	FeO(W)	SiO ₂ (C)	Ni _{0.35} Si _{0.65}
CuO(g)	P ₄ S ₅ (g)	Fe ₂ O ₃	SiO ₂ (CR)	NiSi
CuS(g)	S(g)	Fe ₃ O ₄	SiO ₂ (G)	P
Fe(g)	S ₂ (g)	FeO*Cr ₂ O ₃	SiO ₂ (H)	P(B)
FeO(g)	SO(g)	FeO*MoO ₃	SiO ₂ (Q)	P(P)
FeS(g)	SO ₂ (g)	FeO*SiO	SiO ₂ (S)	P(R)
Mn(g)	SO ₃ (g)	*2FeO*SiO ₂	SiO ₂ (T)	P(W)
MnO(g)	S ₂ O(g)	MnO	Cr ₄ C	S
MnS(g)	Si(g)	MnO ₂	Fe ₃ C	Si
Mo(g)	Si ₂ (g)	Mn ₂ O ₃	MnC ₂	
MoO(g)	SiO(g)	Mn ₃ O ₄	MoC	
MoO ₂ (g)	SiO ₂ (g)	MnO*Fe ₂ O ₃	Ni ₃ C	
MoO ₃ (g)	Cr ₂ FeO ₄	MnO*MoO ₃	C	

Appendix B Elemental Analysis of Welding Electrodes

The electrodes used in this study were analyzed by an outside lab for their respective compositions. The analysis was only performed for the elements listed in table 6.1. The details of the analysis can be found in the attached sheet from Luvak Inc., the facility that conducted these tests.

Luvak Inc., 722 Main Street, P.O. Box 597, Boylston, MA 01505

Analytical No.: 0-16528 Massachusetts Institute of Technology

Method Summaries

Oxygen is determined by inert gas fusions using a Leco model TC-136 oxygen / nitrogen analyzer. In this technique the material is fused in a graphite crucible in an inert atmosphere. Any oxygen present in the sample combines with the carbon from the crucible to form carbon monoxide. This gas is then passed through a copper oxide catalyst to convert it to carbon dioxide. The amount of carbon dioxide present is then measured by infrared detection.

Carbon is analyzed by combustion / infrared detection using a Leco model EC-12 carbon analyzer. In this technique the sample is combusted in a stream of oxygen. Any carbon present in the sample combines with the oxygen to form a mixture of carbon monoxide and carbon dioxide. This mixture is then passed through a platinized silica catalyst to insure complete conversion to carbon dioxide. The amount of carbon dioxide present is then measured by infrared detection.

All remaining elements are analyzed by direct plasma emission (DCP) using a Beckman SpectraSpan VI DCP spectrometer. This technique measures the intensity of the energy produced as an element undergoes transformation from excited to ground state. Because each element emits at a characteristic wavelength, this energy is separated and measured with the aid of a monochromator system and photomultiplier tubes. The source of the excitation is the direct current plasma. Excitation occurs as the sample is pumped as an aerosol into this plasma. Prior to DCP analysis, the sample is dissolved in an acid mixture and diluted to a specified volume. Standard solutions are prepared and run to establish calibration curves. The sample solutions is then run and compared with these calibration curves. All results are expressed as weight percent.

Joseph P. Flanagan
5/7/97

Appendix C Analysis for Welding Fume Composition

Welding fume was collected for elemental analysis of the metal content on Nuclepore filters. A chemical analysis of these samples was performed by the Trace Metals Lab at the Harvard School of Public Health. The procedure involved weighing of the filters (before and after collection), followed by digestion by the Parr Bomb technique and then analysis by inductively coupled plasma - mass spectroscopy (ICP-MS). The details of these subsequent steps are given in the following pages.

Sediment Microwave Digestion Technique

Method for: PARR BOMB MICROWAVE SEDIMENT DIGESTION

Developed by: UMASS/Boston, Env. Sci. Trace Metal Lab

Introduction

Read the Parr instruction manual and bulletin before beginning.

The procedure described was developed for the specific sample weights, acid volumes, and heating times given. Any modification should be made gradually by changing one parameter at a time.

The acid combination given below works best for fine grain sediment samples (100 mesh = 150 μm) with low organic content. Digestion of a 500 μm fraction sample with high organic content has been done but leaves a noticeable organic residue. In any case total sample weight should not greatly exceed 0.2 grams (0.18 - 0.21 grams) to insure complete digestion.* Smaller sample weights will result in increased pressure during heating. Organic samples or samples with a high organic content should be predigested or an alternate procedure should be developed due to the fact that gasses released during digestion of organic material may contribute to excessive pressure build-up.

* We have successfully weighed up to 0.35 grams of sediment without problems and with excellent reproducibility of results. Each sediment type should be considered individually.

Procedure

You will need the following to carry out the procedure:

- Parr bombs
- 45 ml teflon bomb liners with lids and O-rings
- acid cleaned spatula for weighing out sediment
- kimwipes, gloves
- HNO_3 (reagent grade)
- HF (reagent grade)
- 1.5% Boric acid (30.456 grams to 2000 ml DI HOH)
- 125 ml plastic bottles for sample (cleaned in 10% HCl bath)
- pipettes, graduated cylinders
- appropriate sediment reference standard (from NIST or NRCC)
- Microwave oven w/ carousel
- Plastic bucket with lid to hold 4 bombs
- Shallow tub for cooling bombs

1. Assemble clean 45 ml. teflon bomb liners with o-rings and lids. Make sure the lids fit securely into the liner (trying different o-rings with different liners is sometimes useful). Place in a plastic bag to keep clean.
2. Collect liners, spatula, kimwipes, gloves, sediment, notebook, and pen together and proceed to the Mettler analytical balance.
3. Turn balance on and calibrate it according to the procedures described in the instruction manual. Take the lid off one liner and place it on a kimwipe. Place liner on the balance and tare. Carefully add sediment with the spatula to the liner by tipping the liner with one hand and carefully introducing the sediment to the bottom of the liner. This is important because static electricity will attract the sediment to the walls of the liner and you do not want particles around the top of the liners. Weigh out approximately 0.20 - 0.35 grams of sediment (to 4 decimal places), depending on the specifics of your sediment. Write down sample ID, weight, and liner number in the notebook.
4. Remove liner from balance and cap it. Wipe spatula clean with a kimwipe. Repeat procedure until all sediment samples are weighed.

SRM's - Carry at least 10% of appropriate matrix reference material (NIST sediment reference material for trace metal analysis) in the same procedure explained 1 through 4.

5. Proceed to the Class 100 fume hood (in which plastic wrap has been put down), and carefully open the liners. If the o-rings come off the lids and remain in the liner, carefully replace the o-ring on the lid. Add 5 ml HNO₃ and 2 ml concentrated HF.

BLANKS - Carry at least 10% procedure blanks (not less than 2 in number) by adding 5 ml superpure HNO₃ and 2 ml superpure concentrated HF to empty to the teflon liner.

6. Place caps on liner and place liners in bomb casings. Screw on the lid of the casing until snug. Do not over tighten. Place bombs in the plastic container and snap on the lid. Four casings should fit at once. Four bombs should always be run together. If you do not have 4 samples to digest, fill enough liners with about 10 ml of water to bring the total number of bombs up to 4. This is necessary so that the heat is evenly distributed and an explosion is avoided.
7. Place the plastic container on the microwave carousel and heat at approx. 750 Watts (80% power on a 900 W oven) for 3 minutes (this may have to be adjusted for different sediments or different microwaves). Stand back from the microwave oven in case of 'explosion' due to excessive pressure build-up inside the bombs.

Note: If bomb failure occurs during heating, a popping sound or other type of sound may be heard. In such cases the lid of the plastic container may be blown off from leaking acid fumes. Open the microwave door cautiously.

8. Remove the plastic container from the microwave and place it in the hood. Carefully remove the lid. Acid fumes may be seen collected in the bottom of the container. Fan the container lid if necessary.
9. Remove the bombs and place them in a shallow tub in the sink with running cold water. Water should not be above the screw threads of the casing cover. Allow to cool in the water bath for a minimum of 1 hour.
10. Remove the bombs from the water bath. Carefully unscrew the lids in case of residual pressure. Remove the lids from the liners, being careful not to spill or contaminate the sample. Add 10 ml of 1.5% boric acid. Replace caps on the liners, place the liners in the bombs, screw on bomb lids, place into plastic container, snap on lid, and place in the microwave oven. Heat at 750 Watts for 2 minutes.
11. Cool bombs in water bath for 30 minutes - 1 hour.
12. Dilute samples to 50 or 100 ml final sample volume with 1.5% boric acid. Place sample in 125 ml plastic bottle by consecutive rinses and transfers of the sample and acid.
13. For analysis of metals other than As, Se, and Hg, run samples directly on the ICP-MS with external standard calibration corrected with internal standards (See ICP-MS SOP for details).
14. For Mercury analysis, refer to the Mercury Analysis SOP.

Sample extracts and digestates are analyzed for metals on a Perkin-Elmer ELAN 5000 Inductively Couple Plasma - Mass Spectrometer (ICP-MS). The detection limit of an ICP-MS are generally 10 times lower than GFAAS and 100-1000 times lower than ICP-Emission. A calibration curve of external standards is prepared for each analytical run, and Iridium and Indium are used as internal standards to correct for drift in the instrument response. A reference solution provided by the National Institute for Standards and Technology (NIST #1643d) is run after every 10 samples to check for drift in the calibration of the instrument. For each element, the calibration is based on the most abundant isotope of that element free from analytical interferences. The exception is lead, which is determined as the sum of each isotope of the element (^{204}Pb , ^{206}Pb , ^{207}Pb , and ^{208}Pb) to allow for possible differences in the isotopic composition between the samples and standards. The concentration of metals in each digestate is determined in triplicate.

Appendix D NIOSH method 7600

The NIOSH 7600 is a method for determining the Cr VI content in samples collected on PVC membrane filters. This method was used to evaluate the Cr VI percentage in welding fume samples. The sample were analyzed at DataChem Labs in Salt Lake City, UT. The following pages give the details of this test, as published by NIOSH. Attention is drawn to step 5a on page 87, which might be a possible source of oxidation of Cr III and other species to Cr VI, whereby all the Cr is recorded as Cr VI.

CHROMIUM, HEXAVALENT

7600

Cr(VI) MW: 52.00 (Cr); 99.99 (CrO₃) CAS: 18540-29-9 RTECS: GB6262000

METHOD: 7600, Issue 2

EVALUATION: FULL

Issue 1: 15 May 1989

Issue 2: 15 August 1994

OSHA : 0.1 mg/m³ (as CrO₃)
 NIOSH: 0.001 mg/m³/10 h; carcinogen
 ACGIH: 0.050 mg/m³ (as Cr, soluble); some insoluble chromates are human carcinogens

PROPERTIES: oxidizing agent

SYNONYMS: vary depending upon the compound

SAMPLING		MEASUREMENT	
SAMPLER:	FILTER (5.0- μ m PVC membrane)	TECHNIQUE:	VISIBLE ABSORPTION SPECTROPHOTOMETRY
FLOW RATE:	1 to 4 L/min	ANALYTE:	CrO ₄ ²⁻ -diphenylcarbazide complex
VOL-MIN:	8 L @ 0.025 mg/m ³	EXTRACTION SOLUTION:	0.5 N H ₂ SO ₄ or 2% NaOH-3% Na ₂ CO ₃ (see steps 4 and 5)
-MAX:	400 L	WAVELENGTH:	540 nm; 5-cm path length
SHIPMENT:	routine	CALIBRATION:	standard solutions of K ₂ CrO ₄ in 0.5 N H ₂ SO ₄
SAMPLE STABILITY:	analyze within 2 weeks [1]	RANGE:	0.2 to 7 μ g per sample
FIELD BLANKS:	2 to 10 field blanks per set	ESTIMATED LOD:	0.05 μ g per sample
ACCURACY		PRECISION (S _p):	0.029 @ 0.3 to 1.2 μ g per sample [3]
RANGE STUDIED:	0.05 to 0.2 mg/m ³ [2] (22-L samples)		
BIAS:	- 5.48%		
OVERALL PRECISION (S _{PT}):	0.084 [2]		
ACCURACY:	\pm 18.58%		

APPLICABILITY: The working range is 0.001 to 5 mg/m³ for a 200-L air sample. This method may be used for the determination of soluble Cr(VI) (using 0.5 N H₂SO₄ as extraction solution or insoluble Cr(VI) (using 2% NaOH - 3% Na₂CO₃) [3].

INTERFERENCES: Possible interferences are iron, copper, nickel, and vanadium; 10 μ g of any of these causes an absorbance equivalent to about 0.02 μ g Cr(VI) due to formation of colored complexes. Interference due to reducing agents (e.g., Fe, Fe²⁺) is minimized by alkaline extraction (step 5).

OTHER METHODS: This method combines and replaces P&CAM 169 [1], S317 [2] and P&CAM 319 [3]; the Cr(VI) criteria document [4] contains a method similar to P&CAM 169. Method 7604 is also specific for hexavalent chromium, using ion chromatography for measurement.

REAGENTS:

1. Sulfuric acid, conc. (98% w/w).
2. Sulfuric acid, 6 N. Add 167 mL conc. H₂SO₄ to water in a 1-L flask; dilute to the mark.
3. Sulfuric acid, 0.5 N. Add 14.0 mL conc. H₂SO₄ to water in a 1-L flask; dilute to the mark.
4. Sodium carbonate, anhydrous.
5. Sodium hydroxide.
6. Potassium chromate.
7. Diphenylcarbazide solution. Dissolve 500 mg sym-diphenylcarbazide in 100 mL acetone and 100 mL water.
8. Cr(VI) standard, 1000 µg/mL. Dissolve 3.735 g K₂CrO₄ in deionized water to make 1 L, or use commercially available solution.*
9. Calibration stock solution, 10 µg/mL. Dilute 1000 µg/mL Cr(VI) standard 1:100 with deionized water.
10. Filter extraction solution, 2% NaOH-3% Na₂CO₃. Dissolve 20 g NaOH and 30 g Na₂CO₃ in deionized water to make 1 L of solution.
11. Nitrogen, purified.

* See SPECIAL PRECAUTIONS.

EQUIPMENT:

1. Sampler: polyvinyl chloride (PVC) filter, 5.0-µm pore size, 37-mm diameter in polystyrene cassette filter holder (FWSB [MSA] or VM-1 [Gelman] or equivalent).
NOTE: Some PVC filters promote reduction of Cr(VI). Check each lot of filters for recovery of Cr(VI) standard.
2. Personal sampling pump, 1 to 4 L/min, with flexible connecting tubing.
3. Vials, scintillation, 20-mL glass, PTFE-lined screw cap.**
4. Forceps, plastic.
5. Spectrophotometer, UV-visible (540 nm), with cuvettes, 5-cm path length.
6. Filtration apparatus, vacuum.**
7. Beakers, borosilicate, 50-mL.**
8. Watchglass.**
9. Volumetric flasks, 25-, 100- and 1000-mL.**
10. Hotplate, 120 to 400 °C.
11. Micropipettes, 10-µL to 1-mL.
12. Centrifuge tubes, 40-mL, graduated, with plastic stoppers.**
13. Buchner funnel.**
14. Pipettes, TD 5 mL.**

** Clean all glassware with 1:1 HNO₃ and rinse thoroughly before use.

SPECIAL PRECAUTIONS: Insoluble chromates are suspected human carcinogens [4]. All sample preparation should be performed in a hood.

SAMPLING:

1. Calibrate the sampling pump with a representative sampler in line.
2. Sample at an accurately known flow rate in the range 1 to 4 L/min for a sample size of 8 to 400 L. Do not exceed 1 mg total dust loading on the filter.
3. Remove the filter from the cassette within 1 h of completion of sampling and place it in a vial to be shipped to the laboratory. Handle the filter only with forceps. Discard the backup pad.

SAMPLE PREPARATION:

NOTE: There are two sample preparation techniques outlined below. For soluble chromates or chromic acid, follow step 4; for insoluble chromate or Cr(VI) in the presence of Fe, Fe²⁺ or other reducing agents, follow step 5.

4. Sample preparation for soluble chromates and chromic acid.
 - a. Remove the blank and sample filters from the vials, then fold and place them into centrifuge tubes.
 - b. Add 6 to 7 mL 0.5 N H₂SO₄ to each tube, cap, and shake to wash all surfaces of the filter. Allow filter to remain in tube 5 to 10 min [6].
 - c. Remove the filter from the tube with plastic forceps, carefully washing all surfaces with an

- additional 1 to 2 mL 0.5 N H₂SO₄. Discard the filters. Start reagent blanks at this point.
- d. Filter the solution through a moistened PVC filter in a Buchner funnel to remove interferences from suspended dust. Collect the filtrate in a clean centrifuge tube. Rinse the bottle, which contained the filter, with 2 to 3 mL 0.5 N H₂SO₄ and pour into the funnel. Rinse the funnel and filter with 5 to 8 mL 0.5 N H₂SO₄.
 - e. Add 0.5 mL diphenylcarbazide solution to each centrifuge tube. Bring the total volume in each centrifuge tube to 25 mL with 0.5 N H₂SO₄. Shake to mix and allow color to develop (at least 2 min but no longer than 40 min. [6]). Transfer the solution to a clean 5-cm cuvette and analyze within 40 min of mixing (steps 9 through 11).
5. Sample preparation for insoluble chromates and for Cr(VI) in the presence of iron or other reducing agents:
- NOTE: If significant amounts of Cr(III) are expected to be present, degas the sample solution by bubbling nitrogen through it for 5 min. before proceeding and purge the headspace above the solution during step 5.a.
- a. Remove the PVC filter from the bottle, place it in a 50-mL beaker, and add 5.0 mL filter extraction solution, 2% NaOH/3% Na₂CO₃. Start reagent blanks at this point. Purge the headspace above the solution with nitrogen throughout the extraction process to avoid oxidation of any Cr(III). Cover the beaker with a watchglass and heat it to near the boiling point on a hotplate with occasional swirling for 30 to 45 min. Do not boil the solution or heat longer than 45 min. Do not allow the solution to evaporate to dryness because hexavalent chromium may be lost owing to reaction with the PVC filter. An indication that hexavalent chromium has been lost in this manner is a brown-colored PVC filter.
 - b. Cool the solution and transfer it quantitatively with distilled water rinses to a 25-mL volumetric flask, keeping the total volume about 20 mL.
NOTE: If the solution is cloudy, filter it through a PVC filter in a vacuum filtration apparatus using distilled water rinses.
 - c. Add 1.90 mL 6 N sulfuric acid to the volumetric flask and swirl to mix.
CAUTION: CARBON DIOXIDE WILL BE EVOLVED CAUSING INCREASED PRESSURE IN THE FLASK. LET THE SOLUTION STAND FOR SEVERAL MINUTES UNTIL VIGOROUS GAS EVOLUTION CEASES.
 - d. Add 0.5 mL diphenylcarbazide solution, dilute to the mark with distilled water and invert several times to mix thoroughly. Pour out about one-half of the contents of the flask, stopper the flask and shake it vigorously several times, removing the stopper each time to relieve pressure.
NOTE: This step releases bubbles of carbon dioxide which otherwise would cause high and erratic readings.
 - e. Transfer an aliquot of the solution remaining in the flask to a 5-cm cuvette and analyze (steps 9 through 11).

CALIBRATION AND QUALITY CONTROL:

6. Calibrate daily with at least six working standards. Transfer 6 to 7 mL 0.5 N H₂SO₄ to each of a series of 25-mL volumetric flasks. Pipet 0 to 0.7 mL of 10 µg/mL calibration stock solution into the volumetric flasks. Add 0.5 mL diphenylcarbazide solution to each and sufficient 0.5 N H₂SO₄ to bring the volume to 25 mL. These working standards contain 0 to 7 µg Cr(VI).
7. Analyze the working standards together with blanks and samples (steps 9 through 11).
8. Prepare a calibration graph [absorbance vs. µg Cr(VI)].

MEASUREMENT:

9. Set wavelength on the spectrophotometer to 540 nm.
10. Set to zero using a 0.5 N H₂SO₄ reagent blank.
11. Transfer sample solution to a cuvette and record the absorbance.
NOTE 1: A sample containing 1.5 µg Cr(VI)/25 mL gives ca. 0.2 absorbance.

NOTE 2: If the absorbance values for the samples are higher than the standards, dilute using 0.5 N H₂SO₄, repeat this step, and multiply the resulting absorbance by the appropriate dilution factor.

CALCULATIONS:

12. From the calibration graph, determine the mass of Cr(VI) in each sample, W (μg), and in the average blank, B (μg).
13. Calculate the concentration, C (mg/m³), of Cr(VI) in the air volume sampled, V (L):

$$C = \frac{W - B}{V}, \text{ mg/m}^3.$$

EVALUATION OF METHOD:

P&CAM 169 and S317 are essentially the same method and are suitable for soluble chromate and chromic acid. Method S317 was validated with generated samples of chromic acid mist [2,6], and P&CAM 169 was tested with field samples [1,7]. P&CAM 319 was developed because a method was needed to analyze for insoluble chromates [3]. This method was tested with insoluble chromates in matrices such as paints, primer and ceramic powders [3].

Precision, analytical range, recovery data, etc., for the three methods pooled are as follows:

Total \hat{S}_r :	0.084
Measurement \hat{S} , [1-3]:	0.02 to 0.04
Range [3]:	0.5 to 10 μg/m ³
Collection Efficiency [5]:	94.5%
Sampling Rate [1,3]:	1.5 to 2.5 L/min
Stability (two weeks) [1]:	96% recovery
Acceptable Filters [3]:	FWSB (MSA); VM-1 (Gelman).

REFERENCES:

- [1] NIOSH Manual of Analytical Methods, 2nd. ed., V. 1, P&CAM 169, U.S. Department of Health, Education, and Welfare, Publ. (NIOSH) 77-157-A (1977).
- [2] Ibid, V. 3, S317, U.S. Department of Health, Education, and Welfare, Publ. (NIOSH) 77-157-C (1977).
- [3] Ibid, V. 6, P&CAM 319, U.S. Department of Health and Human Services, Publ. (NIOSH) 80-125 (1980).
- [4] NIOSH (1975) Criteria for a Recommended Standard: Occupational Exposure to Chromium (VI). Cincinnati, OH: U.S. Department of Health, Education, and Welfare, National Institute for Occupational Safety and Health, DHEW (NIOSH) Publication No. 76-129.
- [5] NIOSH/OSHA Occupational Health Guidelines for Chemical Hazards. Occupational Health Guidelines for Chromic Acid and Chromates. U.S. Department of Health and Human Services (NIOSH) Publication No. 81-123 (1981).
- [6] Documentation of the NIOSH Validation Tests, U.S. Department of Health, Education, and Welfare, Publ. (NIOSH) 77-185 (1977).
- [7] Abell, M. T. and J. R. Carlberg. A Simple Reliable Method for the Determination of Airborne Hexavalent Chromium, *Am. Ind. Hyg. Assoc. J.*, 35, 229 (1974).

METHOD REVISED BY:

Martin T. Abell, NIOSH/DPSE; Method S317 validated under NIOSH Contract CDC-99-74-45.

Biography

The author was born in Bangalore in South India. He was raised in a traditional South Indian atmosphere, growing up in an extended family, with grandparents, uncles and aunts contributing to his upbringing. Upon completion of his ninth standard (grade), he migrated to the United States to complete his high school education in Williamsville, NY, a suburb of Buffalo. He adjusted well to the new atmosphere, and later proceeded to the Massachusetts Institute of Technology in Cambridge, MA, to pursue his college studies. He received his bachelors degree in Materials Science and Engineering in February 1995, graduating *Tau Beta Pi* a semester early to obtain his degree in three and a half years. He was part of the co-op program and thus interned at the Ford Motor Company in Dearborn, MI. After completion of his B.S., he spent several months in India directing a summer school project devoted to Indian culture and participating in other family activities. He returned to MIT during the fall of 1995 to start graduate work in Materials Science and Engineering. He served as a teaching assistant for an introductory ceramics course for the first semester, following which he joined the MIT Joining Group to begin the current project. Post-graduation plans are to join MicroStrategy in Vienna, VA, to begin a career in decision support.